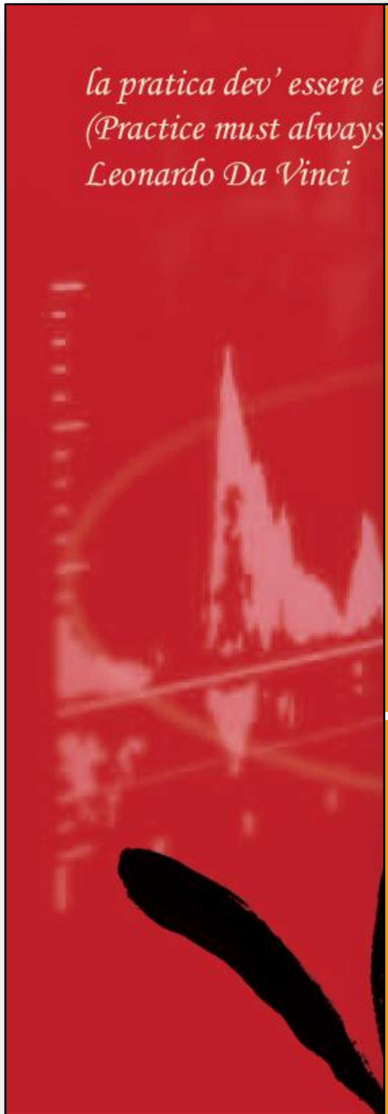

Reconstruc
A practical

Day 1

08.30	Arrival, registration	
09.00	Welcome and introduction	*H.-J. Schäfers*
09.45	Aortic regurgitation and aneurysm- Epidemiology and guidelines	*W. Fehske*
	BREAK	
10.30	Anatomy of aortic valve and root	*M. Heinemann*
11.00	AV repair – the Homburg approach	*H.-J. Schäfers*
11.30	Why and when to repair the aortic valve	*I. El-Hamamsy*
	BREAK	
13.00	Videos root repair	*H.-J. Schäfers*
14.00	Root repair – the Tel Aviv approach	*E. Raanani*
14.20	Echo assessment of AR and its mechanisms	*W. Fehske*
14.40	Repair or Ross operation	*I. El-Hamamsy*
	BREAK	
15.30	The AV junction in aortic repair	*E. Lansac*
16.00	Videos cusp repair	*H.-J. Schäfers*
17.00	Results of cusp and root repair	*C. Giebels*
18.00	Adjourn	

Day 2

07.45	Case presentations	
	Live operations: Moderation E. Raanani	
08.00	Case #1 Root repair	
09.30	Case #2 Root repair	
10.15	Shortcut to echo – intraop. echo and morphology	*F. Langer*
	BREAK	
11.15	Case #3 Root repair	
12.15	Discussion	
	BREAK	
13.00	Reimplantation should be the preferred technique	*E. Raanani*
13.15	Remodeling is my standard approach	*H.-J. Schäfers*
14.00	3-dimensional echo in aortic valve repair	*W. Fehske*
14.30	How to start root repair	*H.-J. Schäfers*
	BREAK	
15.30	Wetlab (bring your loupes!)	*Faculty*
18.00	Adjourn	

3D TEE data aquisition aortic root

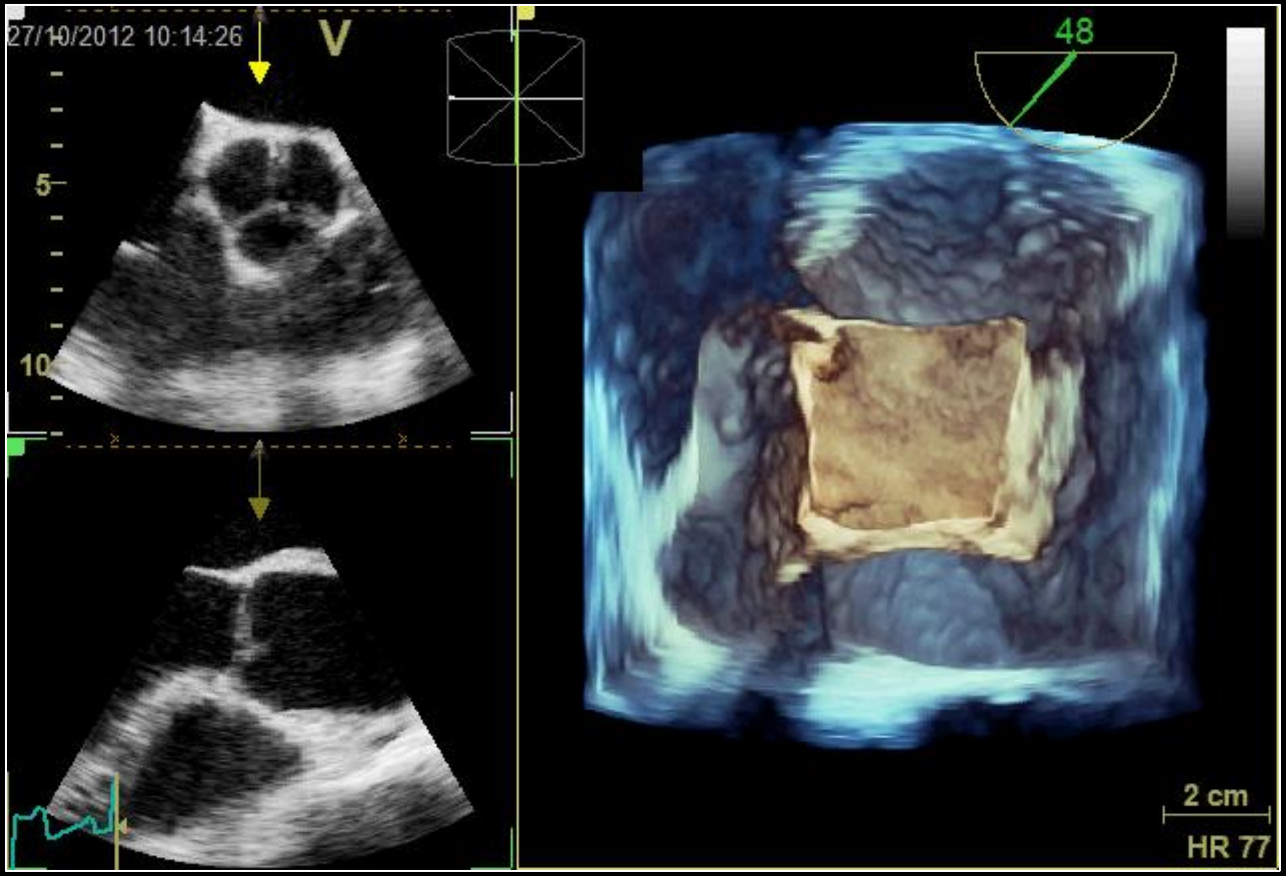

- three orthogonal planes simultaneous
- one plane (to select) 3D surface rendered

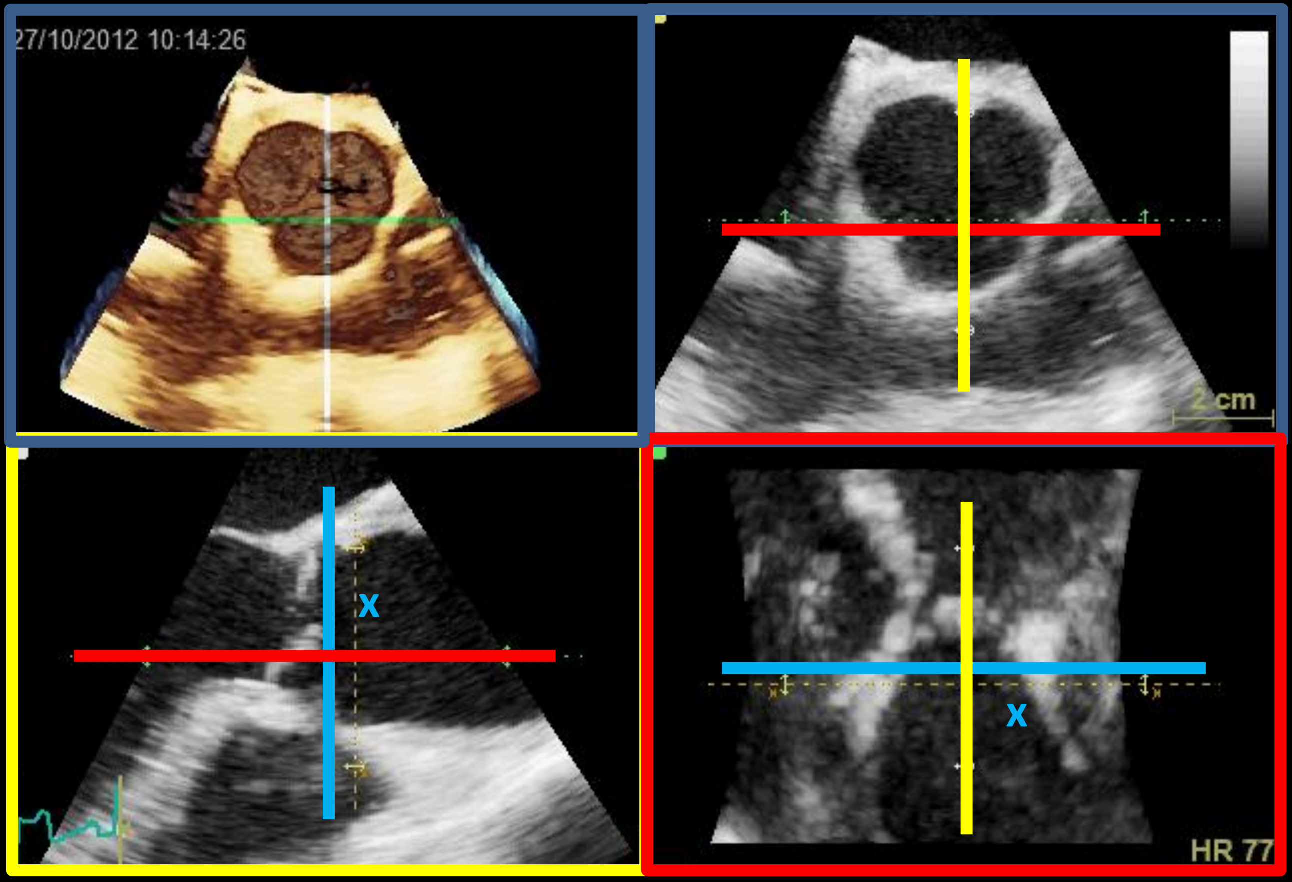

Aortic „ring“ size

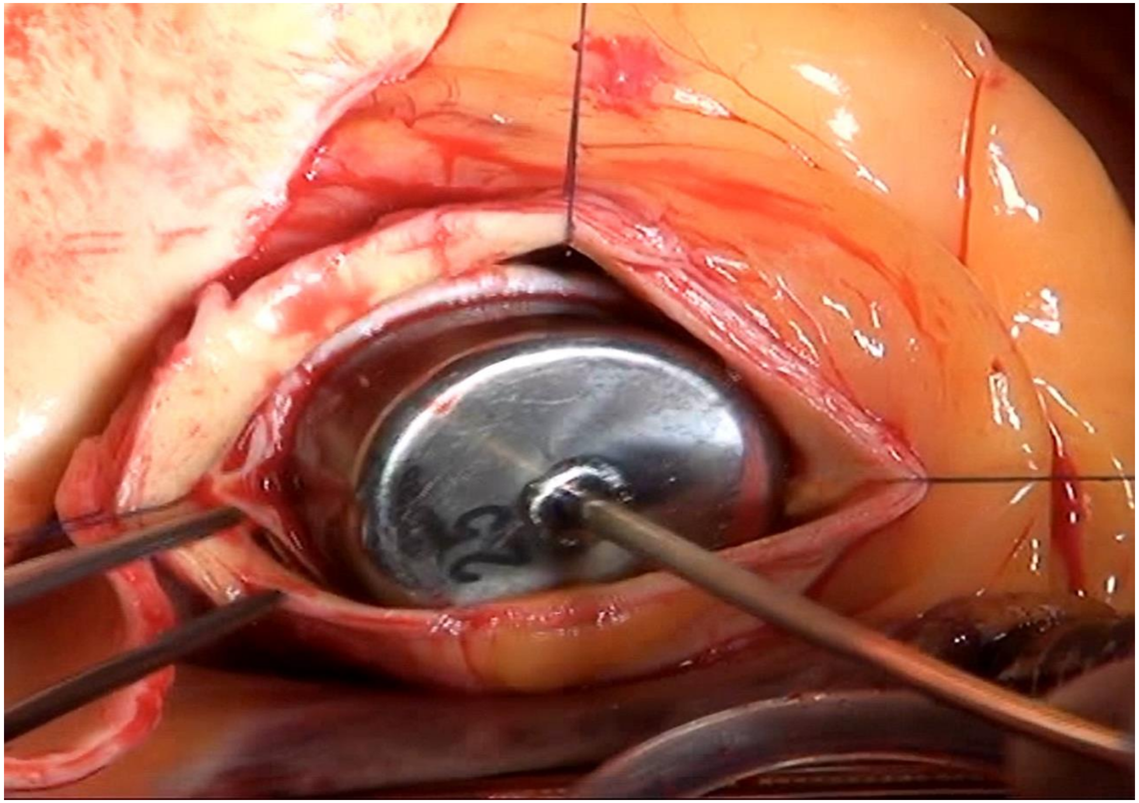

Reconstruction of the Aortic Valve
and Root, Homburg
2013 May 15th/16th/17th Case 2
Prof. Schaefers

Figure 4. A, Three-dimensional arrangement of the aortic root, which contains 3 circular "rings," but with the leaflets suspended within the root in crown-like fashion.

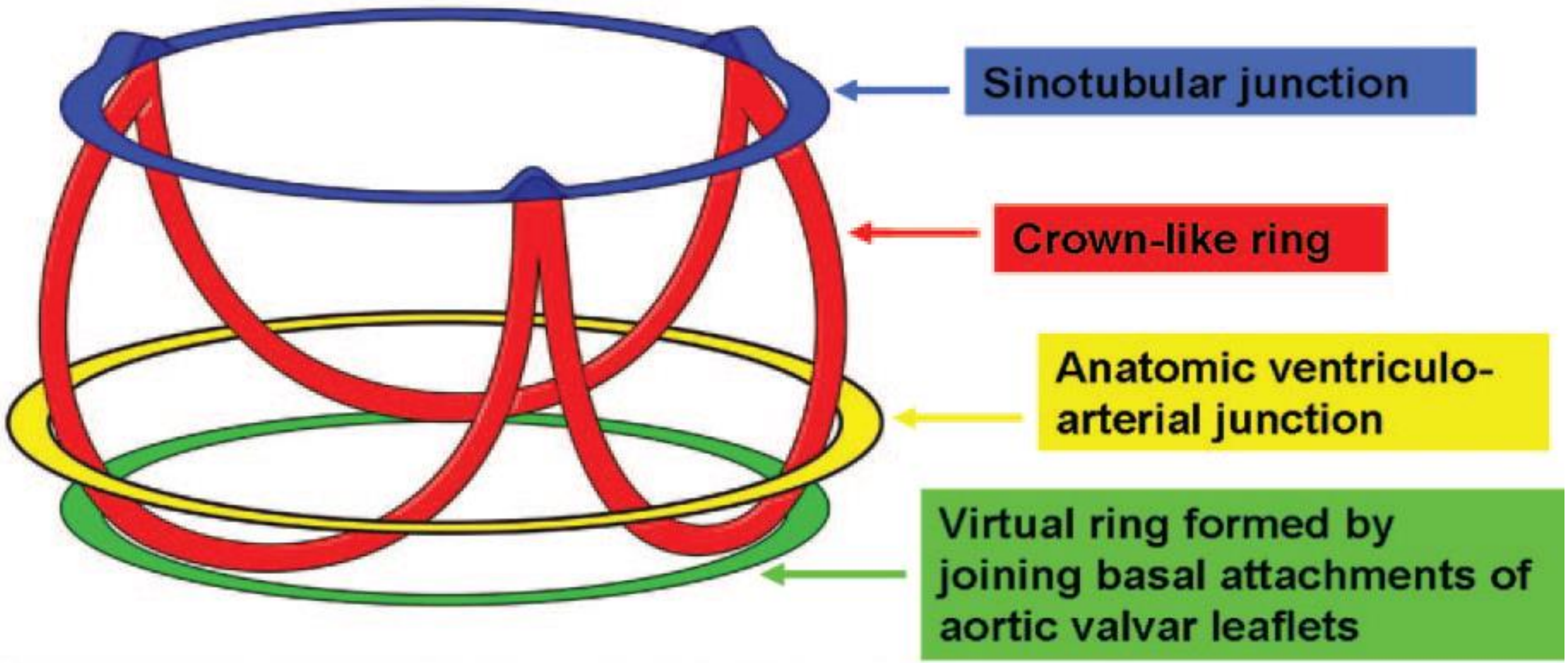

Piazza N et al. Circ Cardiovasc Interv 2008;1:74-81

Rotational and translational movements have to be considered for reliable measurements of the aortic root

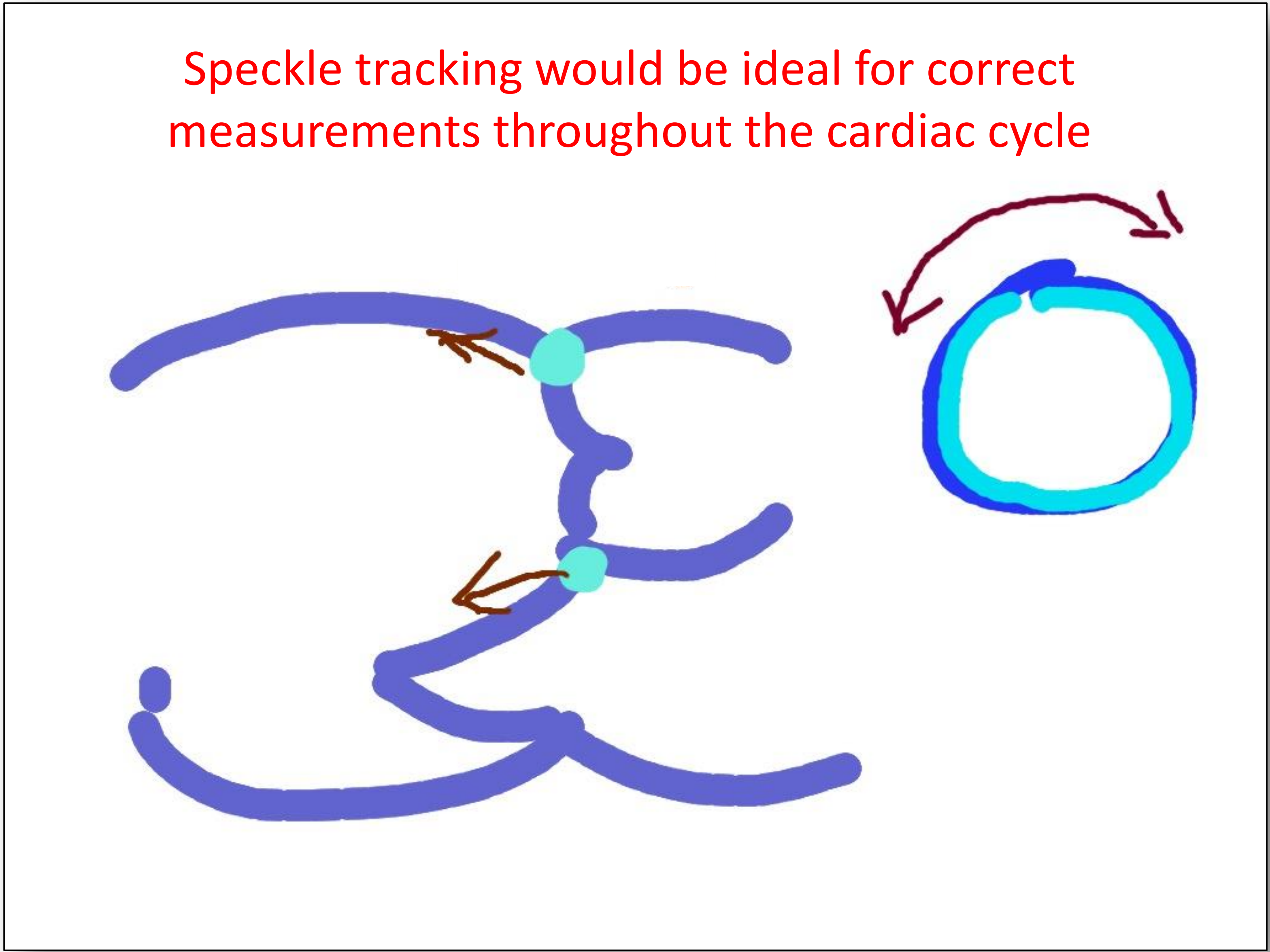

Automated Quantitative 3-Dimensional Modeling of the Aortic Valve and Root by 3-Dimensional Transesophageal Echocardiography in Normals, Aortic Regurgitation, and Aortic Stenosis

Comparison to Computed Tomography in Normals and Clinical Implications

Anna Calleja, MD*; Paaladinesh Thavendiranathan, MD, Msc*; Razvan Ioan Ionasec, PhD; Helene Houle, RDCS, RVT; Shizhen Liu, MD, PhD; Ingmar Voigt, MSc; Chittoor Sai Sudhakar, MD; Juan Crestanello, MD; Thomas Ryan, MD; Mani A. Vannan, MBBS

(*Circ Cardiovasc Imaging*. 2013;6:99-108.)

Automated Quantitative 3-Dimensional Modeling of the Aortic Valve and Root by 3-Dimensional Transesophageal Echocardiography in Normals, Aortic Regurgitation, and Aortic Stenosis

Comparison to Computed Tomography in Normals and Clinical Implications

Anna Calleja, MD*; Paaladinesh Thavendiranathan, MD, Msc*; Razvan Ioan Ionasec, PhD;
Helene Houle, RDCS, RVT; Shizhen Liu, MD, PhD; Ingmar Voigt, MSc; Chittoor Sai Sudhakar, MD;
Juan Crestanello, MD; Thomas Ryan, MD; Mani A. Vannan, MBBS

(*Circ Cardiovasc Imaging*. 2013;6:99-108.)

‘Hinge-to-hinge’ assessment: three predefined standard views were reconstructed to assess of aortic annulus anatomy using multiplanar reformatted images adjusted to the axis of the aortic root.

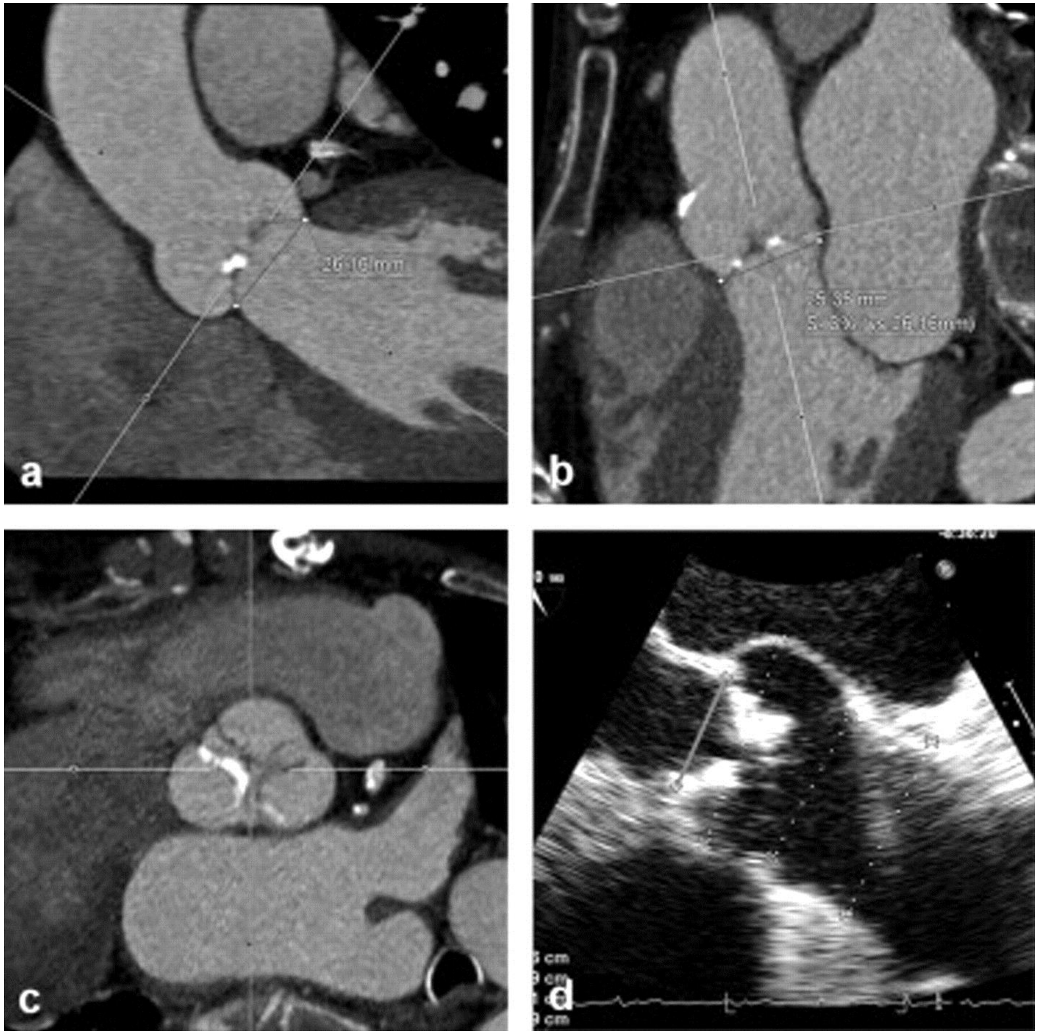

Blanke P et al. Eur J Cardiothorac Surg 2010;38:750-758

EUROPEAN JOURNAL OF CARDIO-THORACIC SURGERY

Cross-Sectional Computed Tomographic Assessment Improves Accuracy of Aortic Annular Sizing for Transcatheter Aortic Valve Replacement and Reduces the Incidence of Paravalvular Aortic Regurgitation

Hasan Jilaihawi, BSc (Hons), MBChB; Mohammad Kashif, MD; Gregory Fontana, MD; Azusa Furugen, MD, PhD; Takahiro Shiota, MD; Gerald Friede, BS, MS; Rakhee Makhija, MD; Niraj Doctor, MBBS; Martin B. Leon, MD; Raj R. Makkar, MD

J Am Coll Cardiol. April 03, 2012,59(14):1275-1286 doi:10.1016/j.jacc.2011.11.045

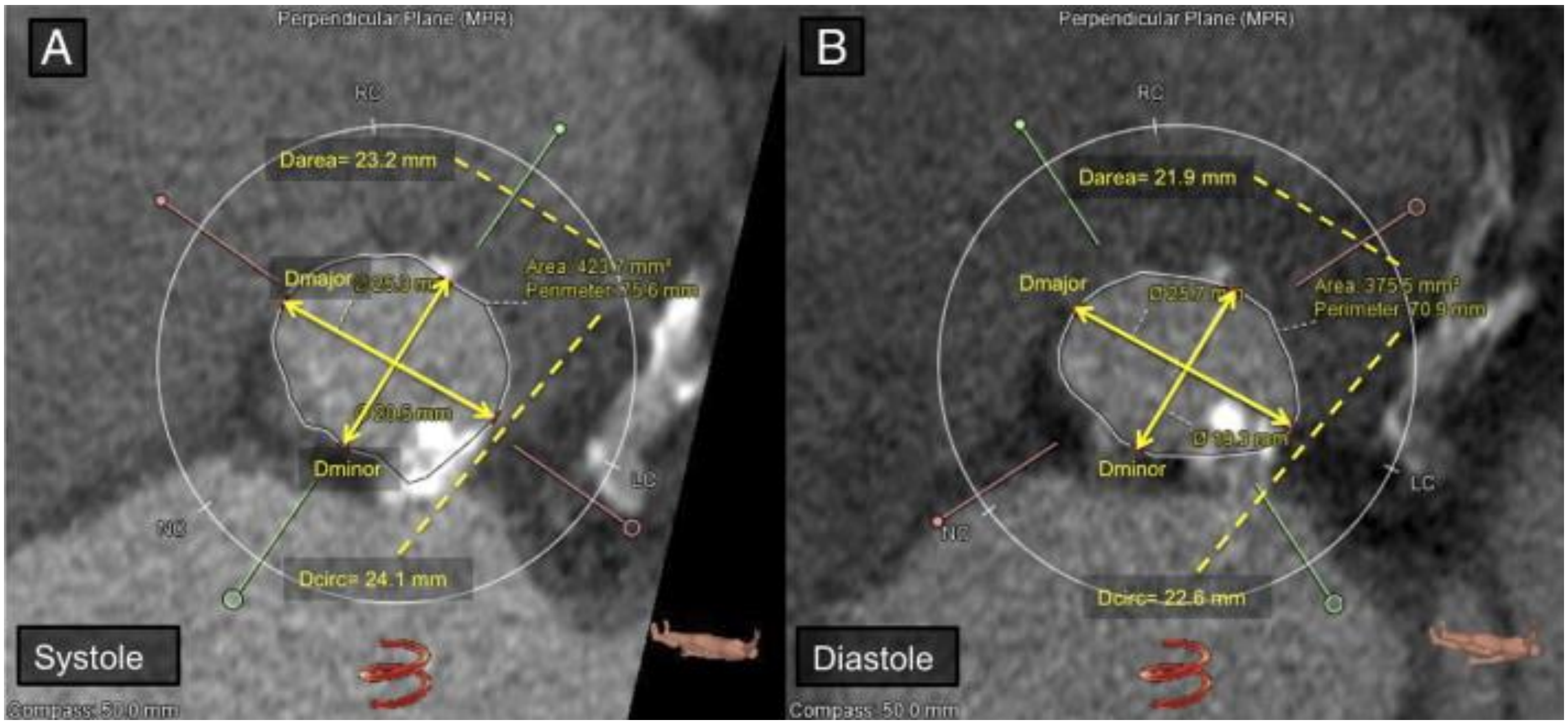

Visualization in fixed planes:

- above the valve

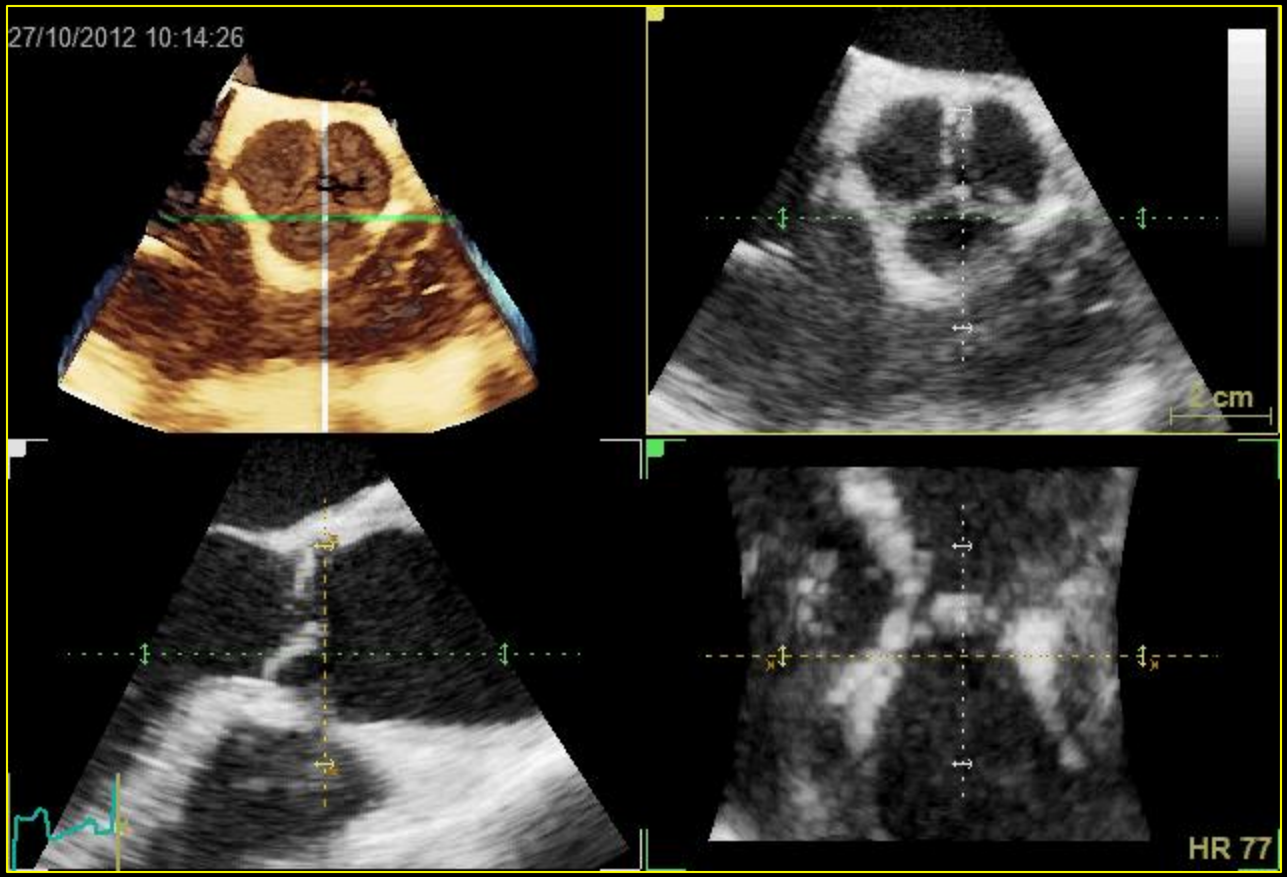

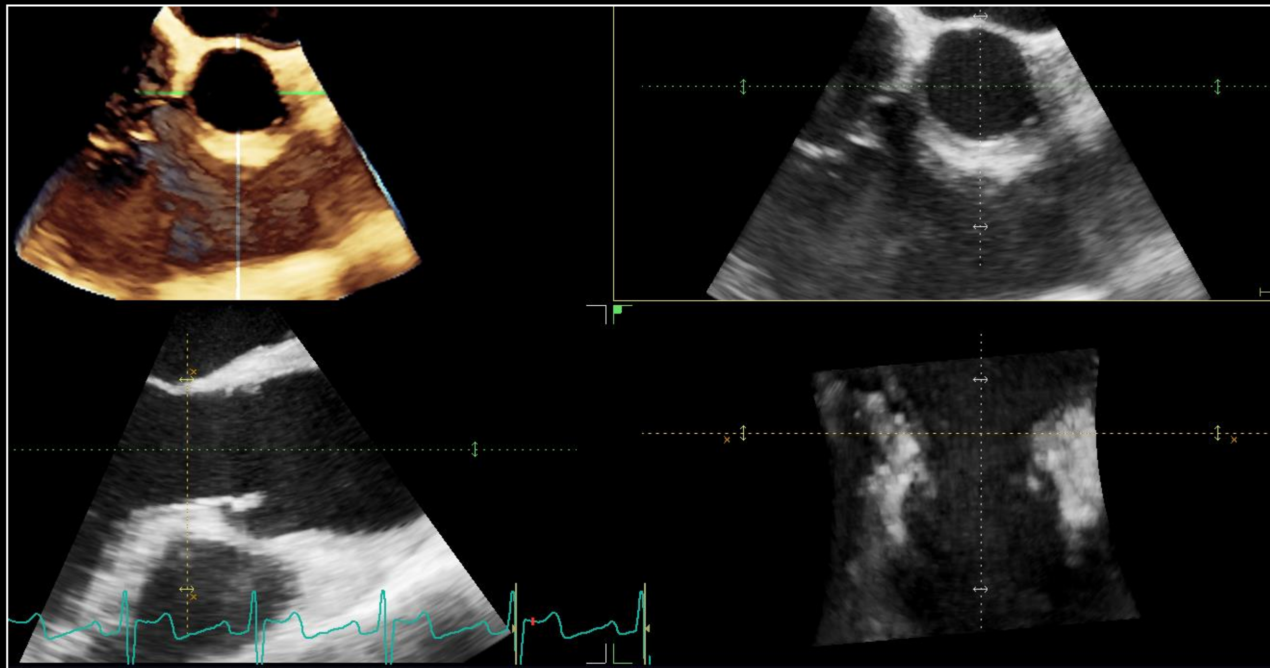

Systole

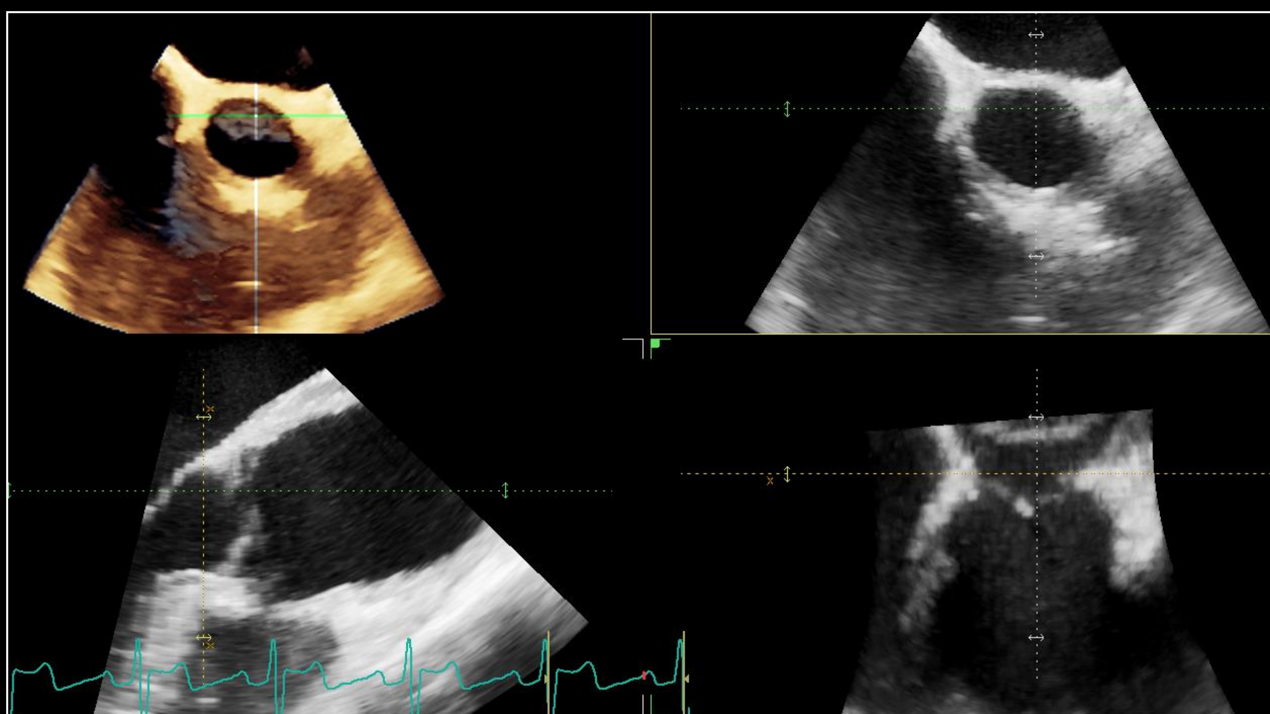

Diastole

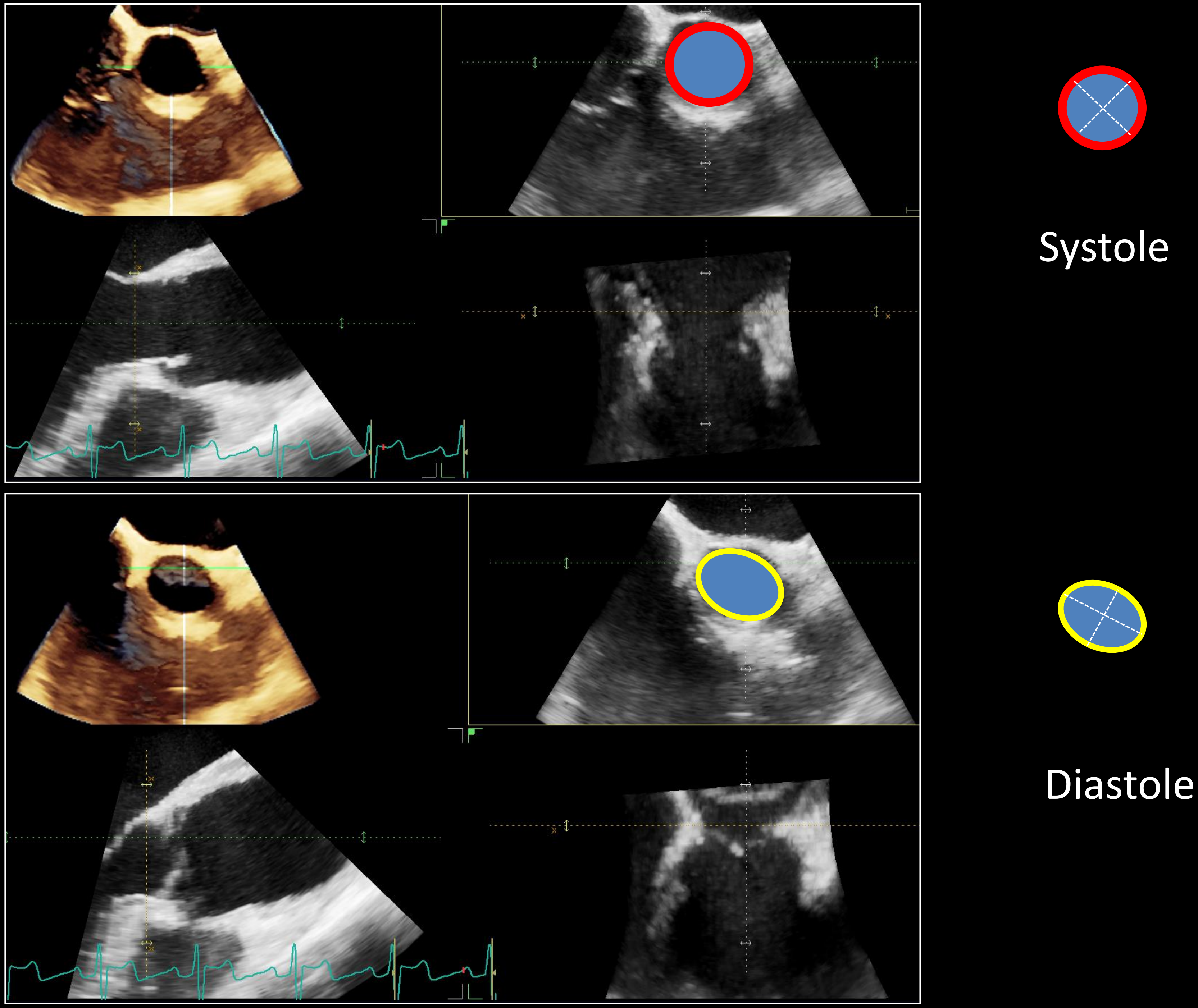
Systole
Diastole

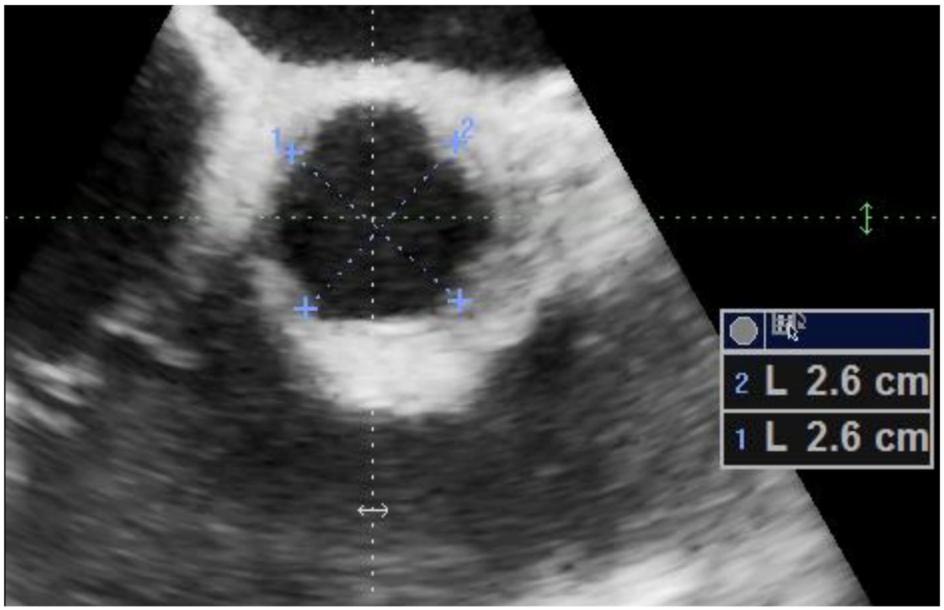

Systole

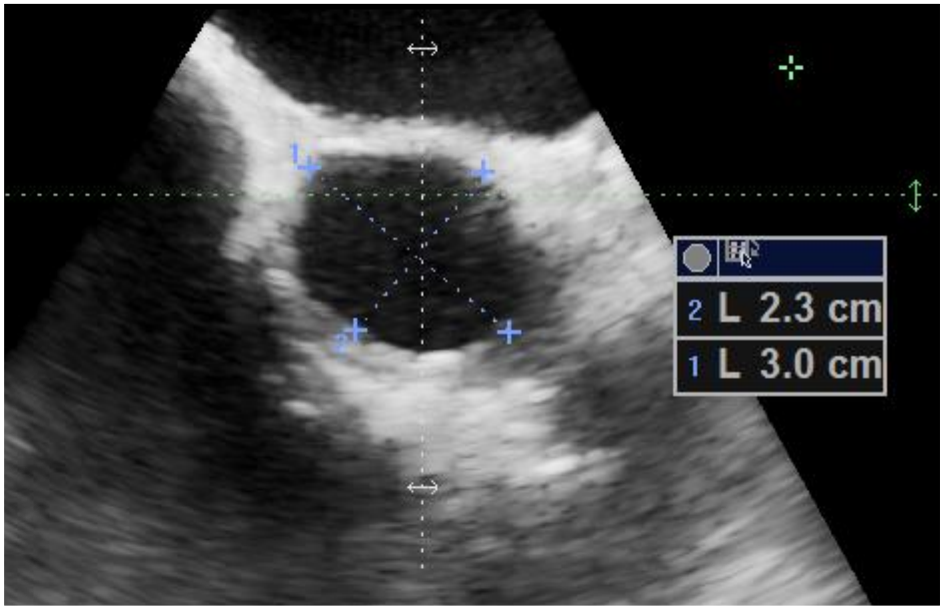

Diastole

Aortico-mitral coupling throughout the cardiac cycle

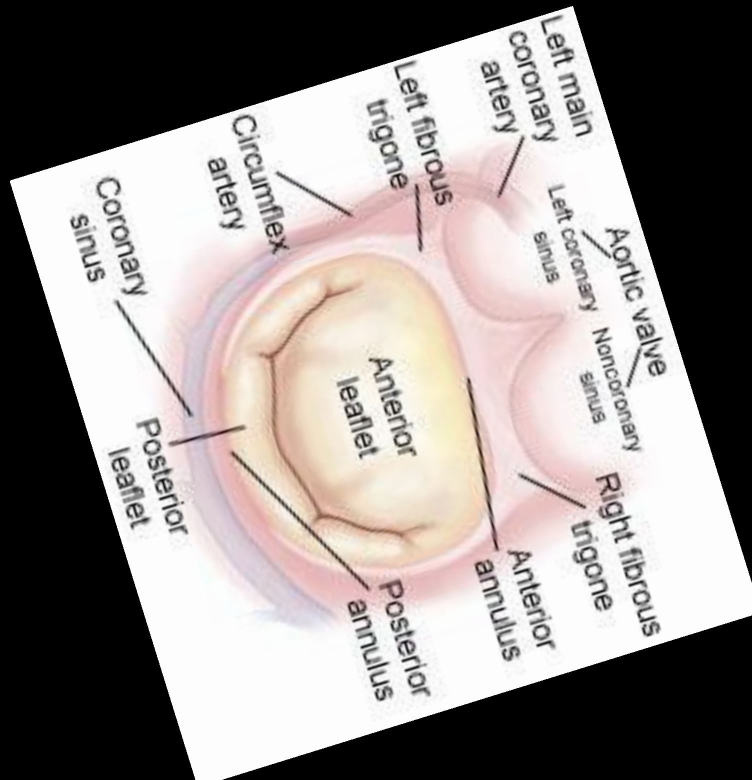

whole cycle

Measuring the aortic root from 3D TEE

W. M.; 86 J., severe AS, planning transfemoral TAVI

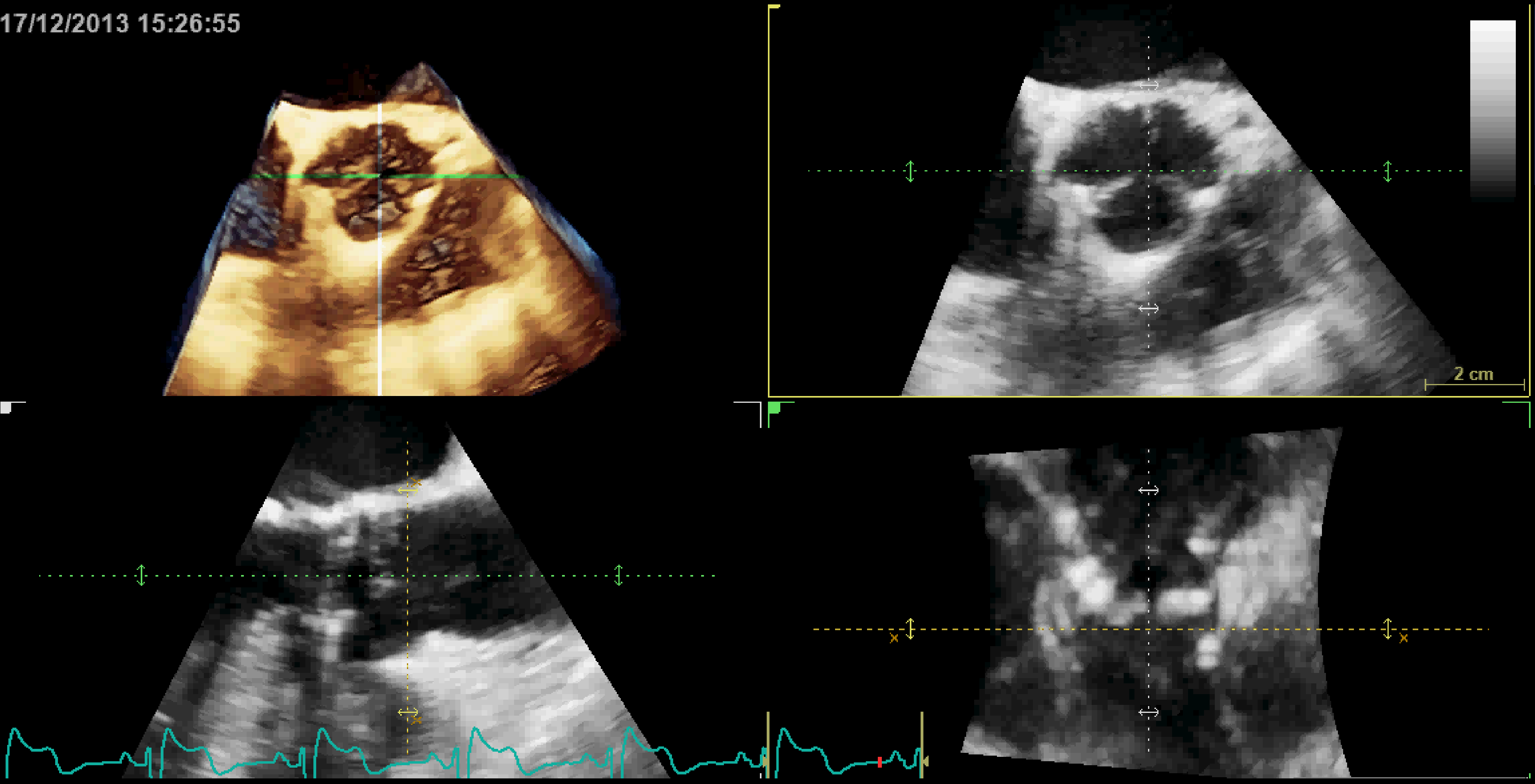

Übersicht durch zentrales Scannen, systolisches Bild:
Planimetrie, ausmessen von vier Diamtern

Vermessung der Aortenwurzel aus dem 3D TEE

W. M.; 86 J., hochgradige symptomatische AS, transfemorale TAVI geplant

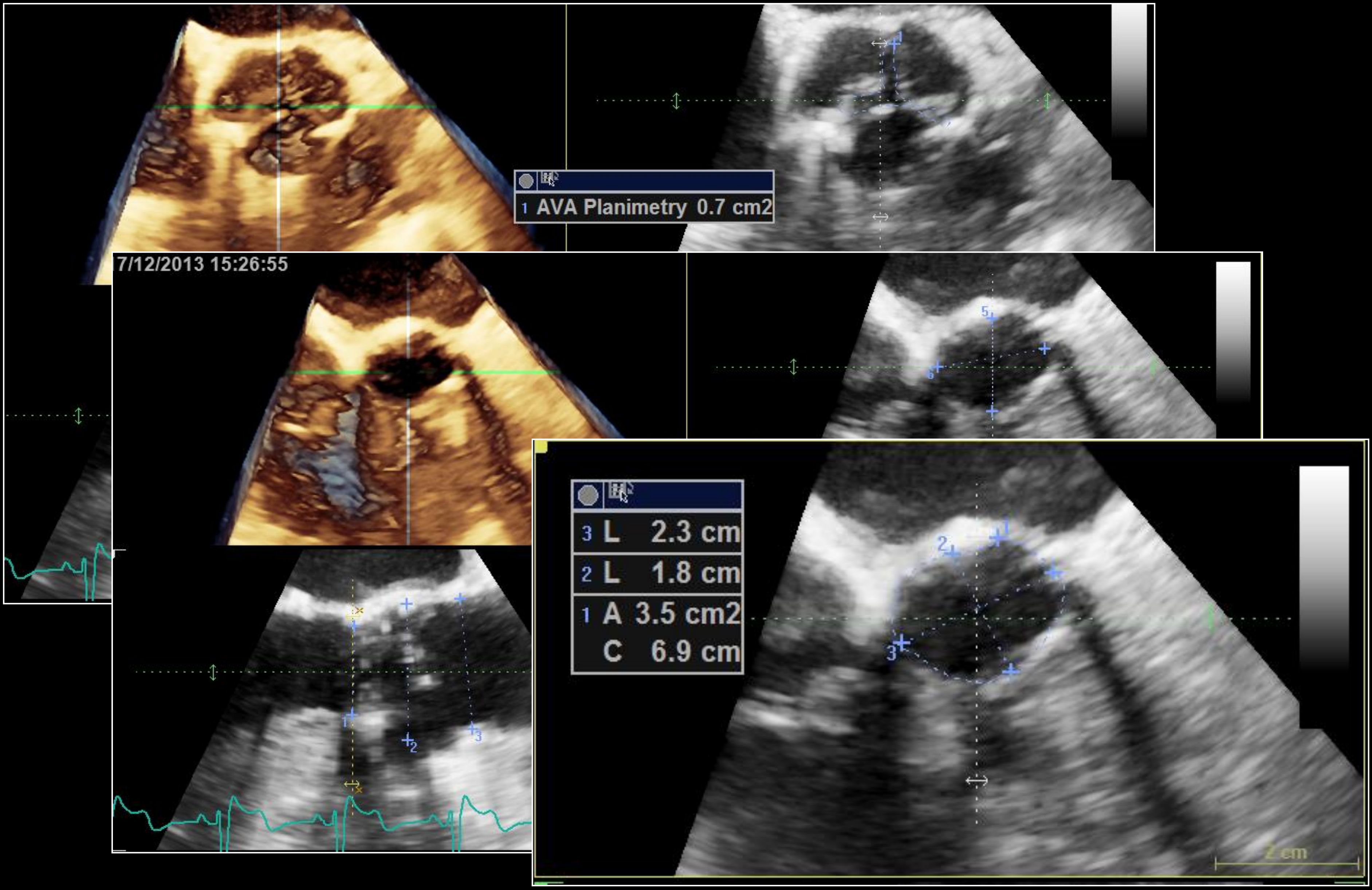

Vermessung der Aortenwurzel aus dem 3D TEE

W. M.; 86 J., hochgradige symptomatische AS, transfemorale TAVI geplant

Bildorientierung „ausnahmsweise“ am CT orientiert,
Ansicht vom LVOT und anterior vorne

Vermessung der Aortenwurzel aus dem 3D TEE

W. M.; 86 J., hochgradige symptomatische AS, transfemorale TAVI geplant

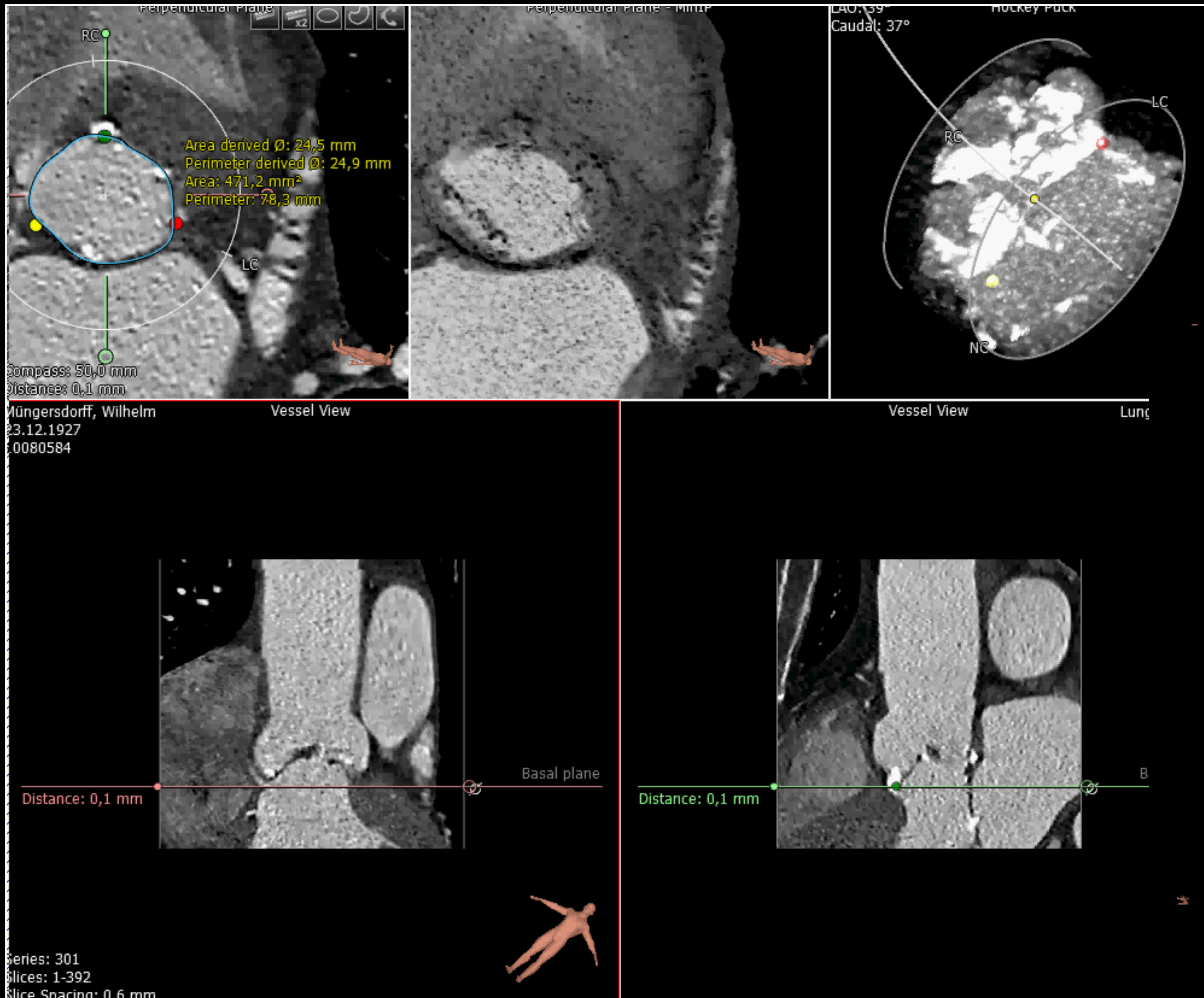

Halbautomatisierte CT-Vermessung der Aortenwurzel 3mensio®

Vermessung der Aortenwurzel aus dem 3D TEE

W. M.; 86 J., hochgradige symptomatische AS, transfemorale TAVI geplant

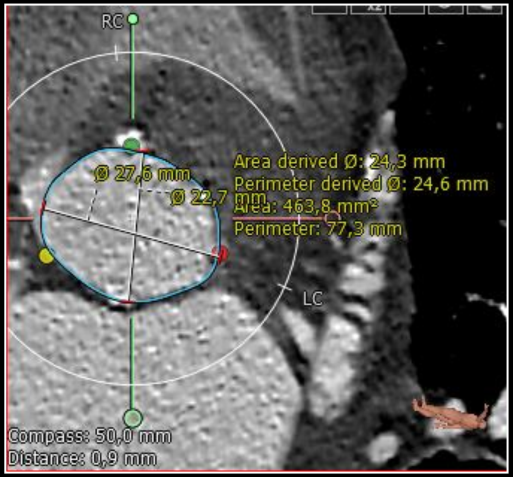

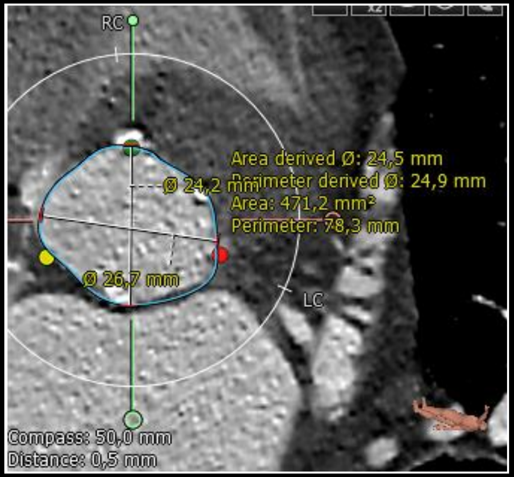

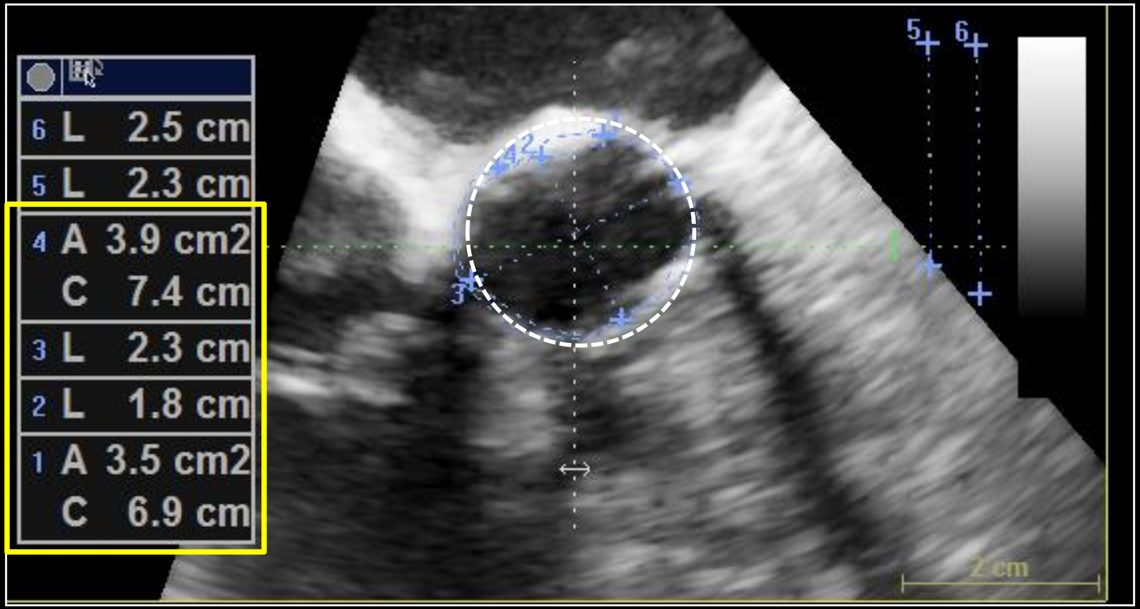

Halbautomatisierte CT-Vermessung der Aortenwurzel 3mensio®

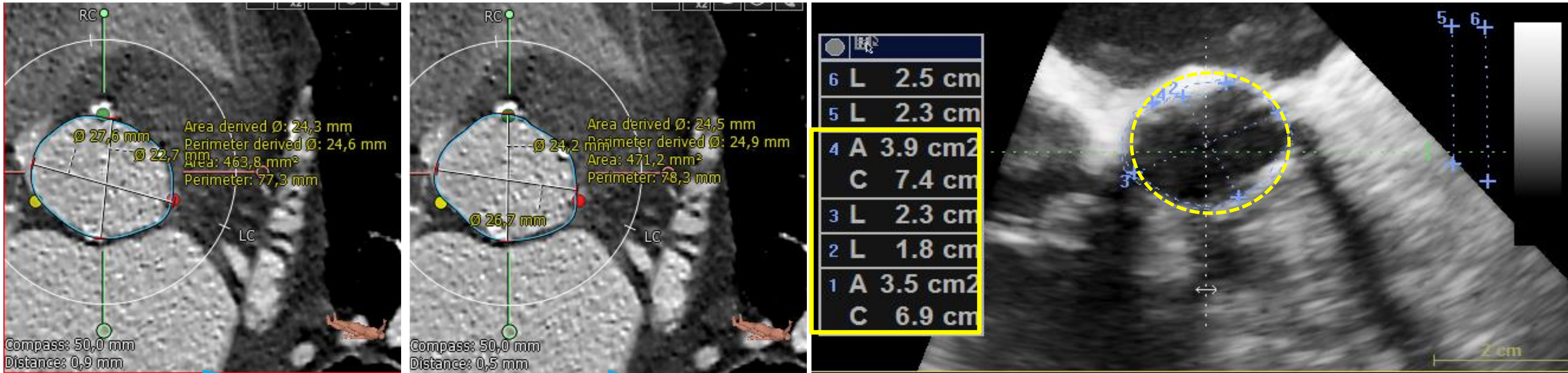

	CT 3mensio (1)	CT 3mensio (2)	3D TEE (1)	3D TEE (2)
area virtual ring	463,8	471,2	350,0	390,0
circumference virtual ring	77,3	78,3	69,0	74,0
D_{area}	24,3	24,5	21,1	22,3
D_{circ}	24,6	24,9	22,0	23,6
D_{max}	26,1	26,6	22	23,0
D_{min}	18,8	18,6	19	19,0
$D_{long\ axis}$			20	21,0
$D_{frontal\ plane}$			21	21,0

circle area $= \pi \times (D/2)^2$

$D_{area} = 2 \times \sqrt{\text{circle area}/\pi}$

circle circumference $= D \times \pi$

$D_{circ} = \text{circle circumference} / \pi$

Vermessung der Aortenwurzel:
Vergleich zwischen CT und 3D-TEE
- Vorhersehbarkeit paravalvulärer Lecks (?)

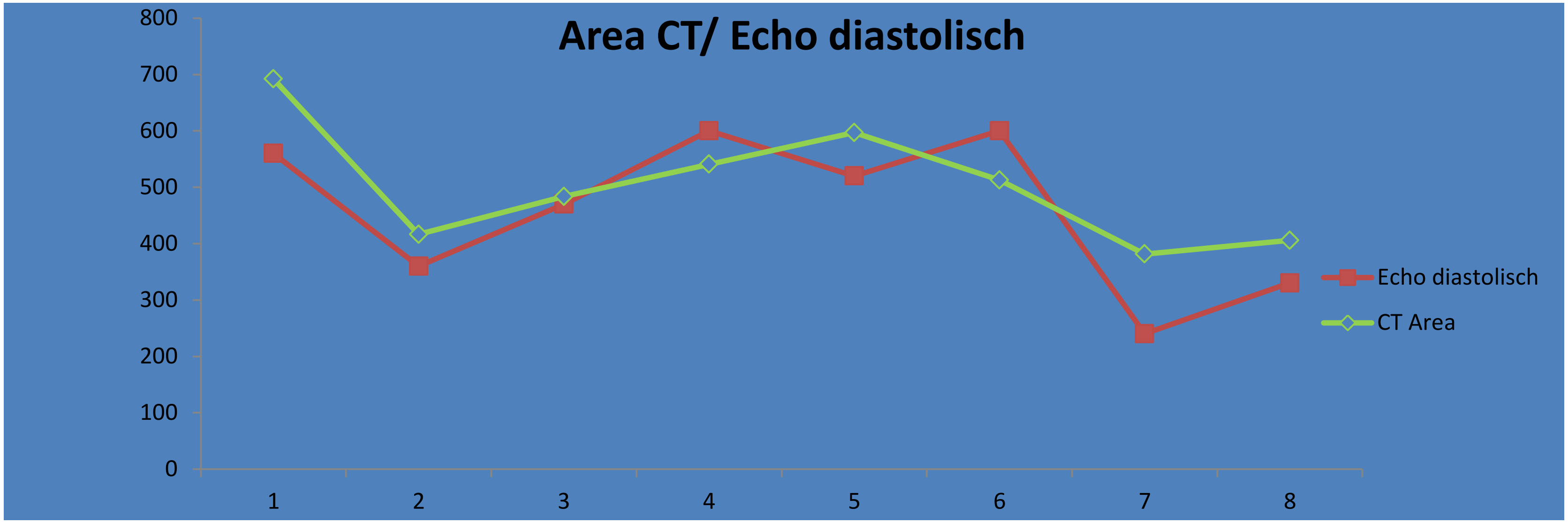

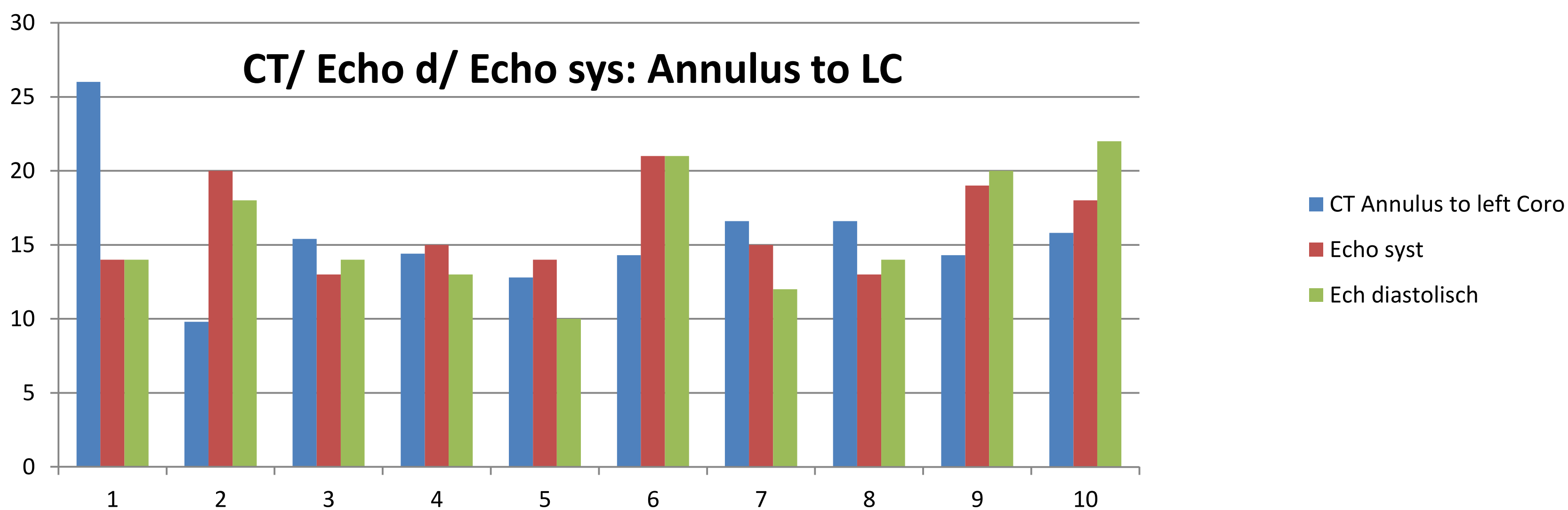

Masters of Cardiothoracic Surgery

Valve sparing root replacement: the remodeling technique with external ring annuloplasty

Emmanuel Lansac[1], Isabelle Di Centa[2], Jan Vojacek[3], Jan Nijs[4], Jaroslav Hlubocky[5], Gianclaudio Mecozzi[6], Mathieu Debauchez[7]

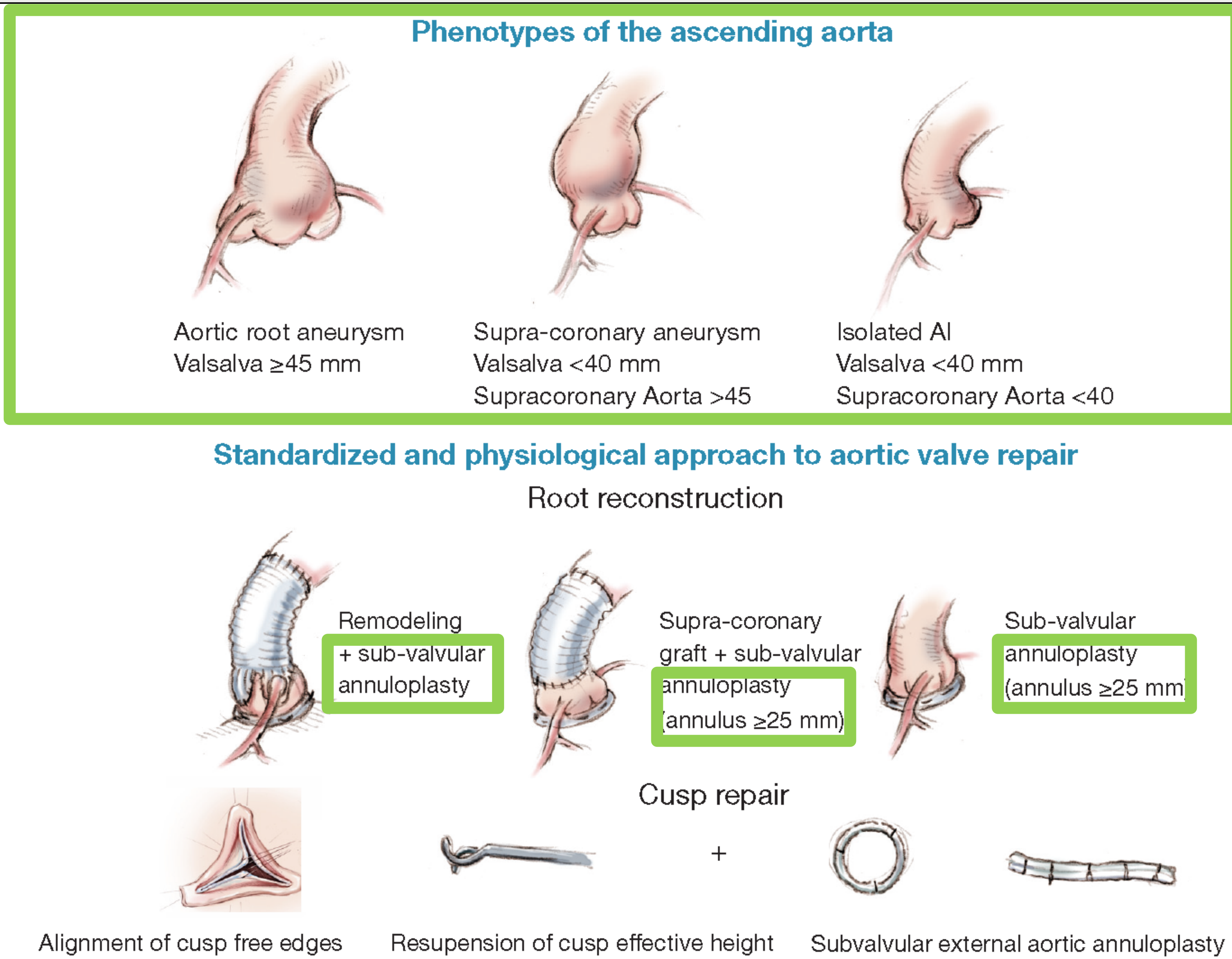

Figure 7 Standardized and physiological approach to aortic valve repair according to each phenotype of ascending aorta

Practical approach for decision making in AR and diseases of the ascending aorta

D. Aicher, H.J. Schaefers

Isolated aortic valve reconstruction (a: plication; b: triangular resection; c: pericardial patch) – normal sinus diameter(<40mm) and normal sinutubular junction (<33mm)

Supracommisural replacement of ascending aorta – dilated sinutubular junction (>33mm) and normal dimension of sinus (<40mm)

Aortic root remodeling (Yacoub) – dilated sinus (>40mm) and dilated sinutubular junction (>33mm)

Dilated basal ring (>25mm) additional annuloplasty in all reconstruction modalities

Aim of each reconstruction: normalisation of dimensions of Aorta adequate configuration of cusps (effective height 10 mm).

LEIPZIG-DALLAS

Echocardiographic **predictors of successful AV repair**

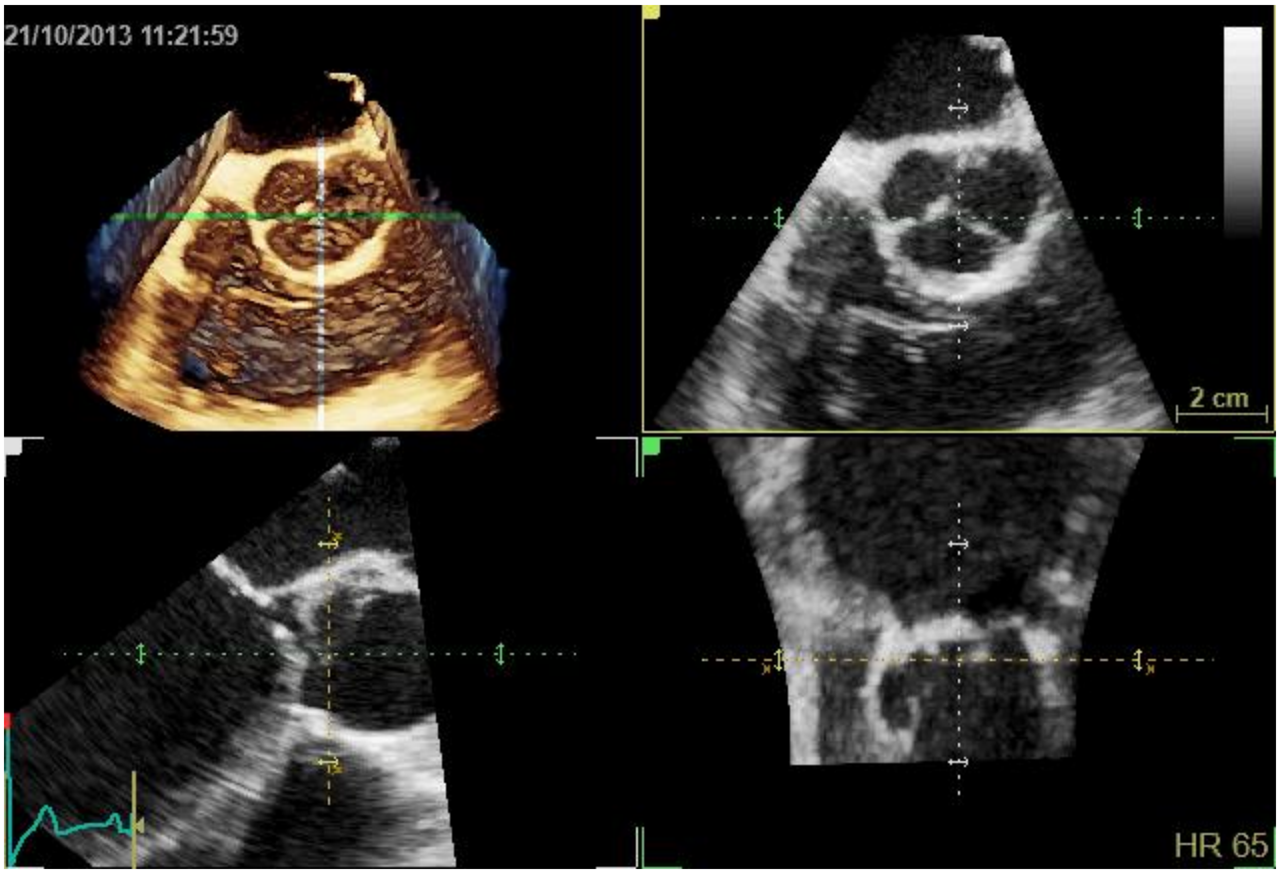

56 y, m, asymptomatic AR III

Surgical examination of the valve

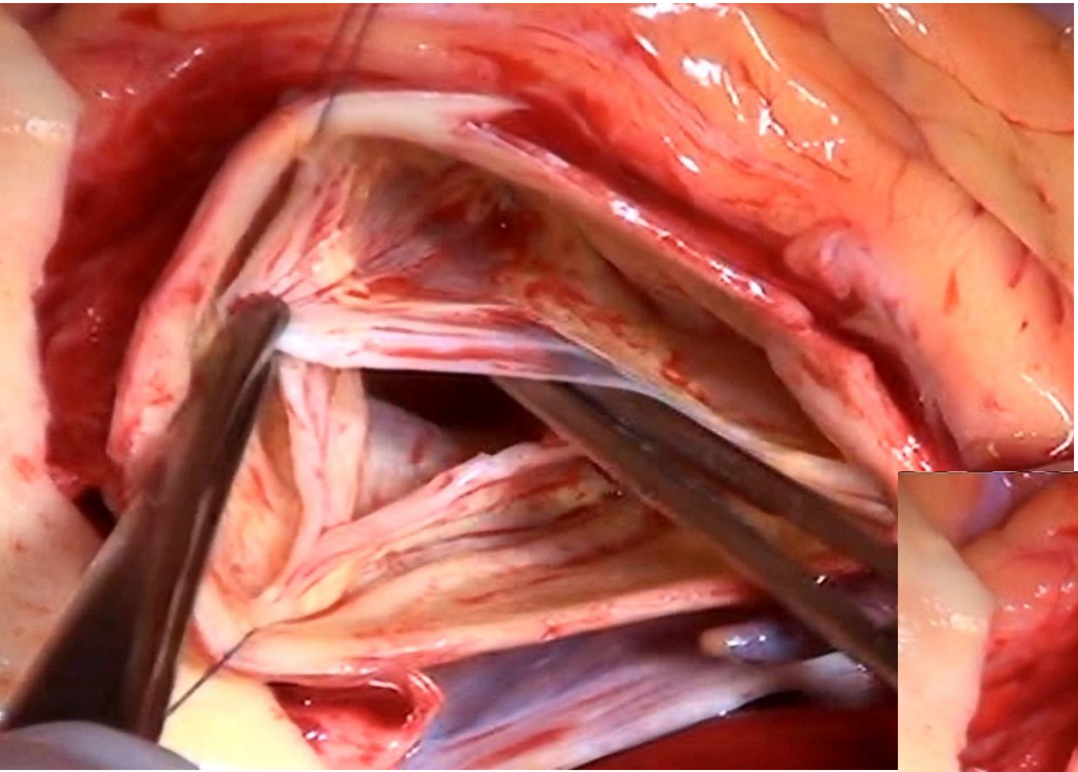

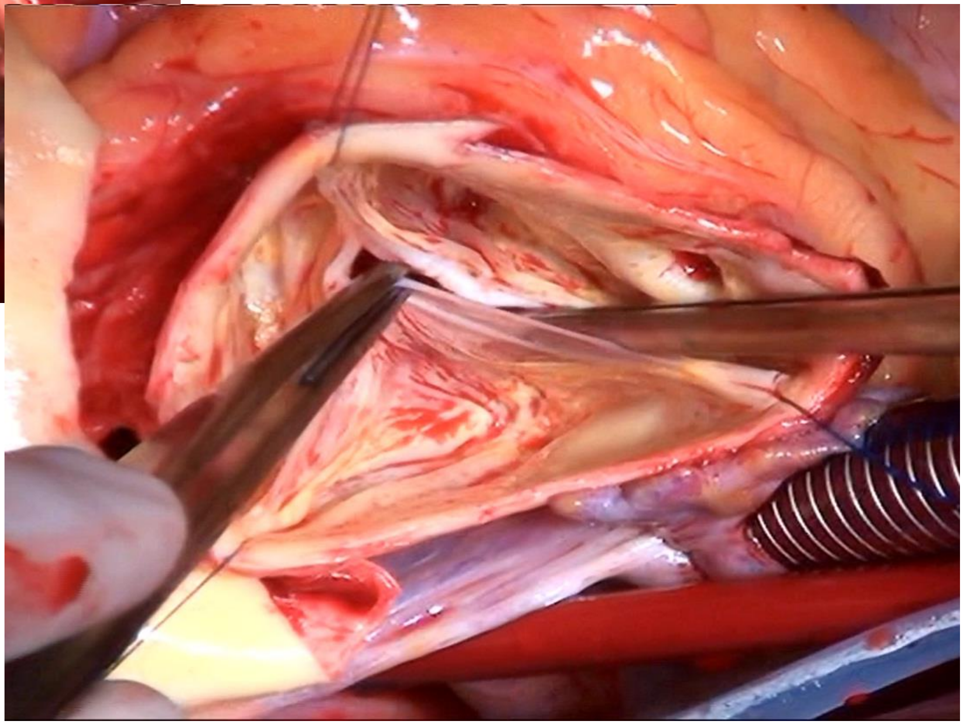

Reconstruction of the Aortic Valve and Root, Homburg
2013 May 15th/16th/17th Case 2
Prof. Schaefers

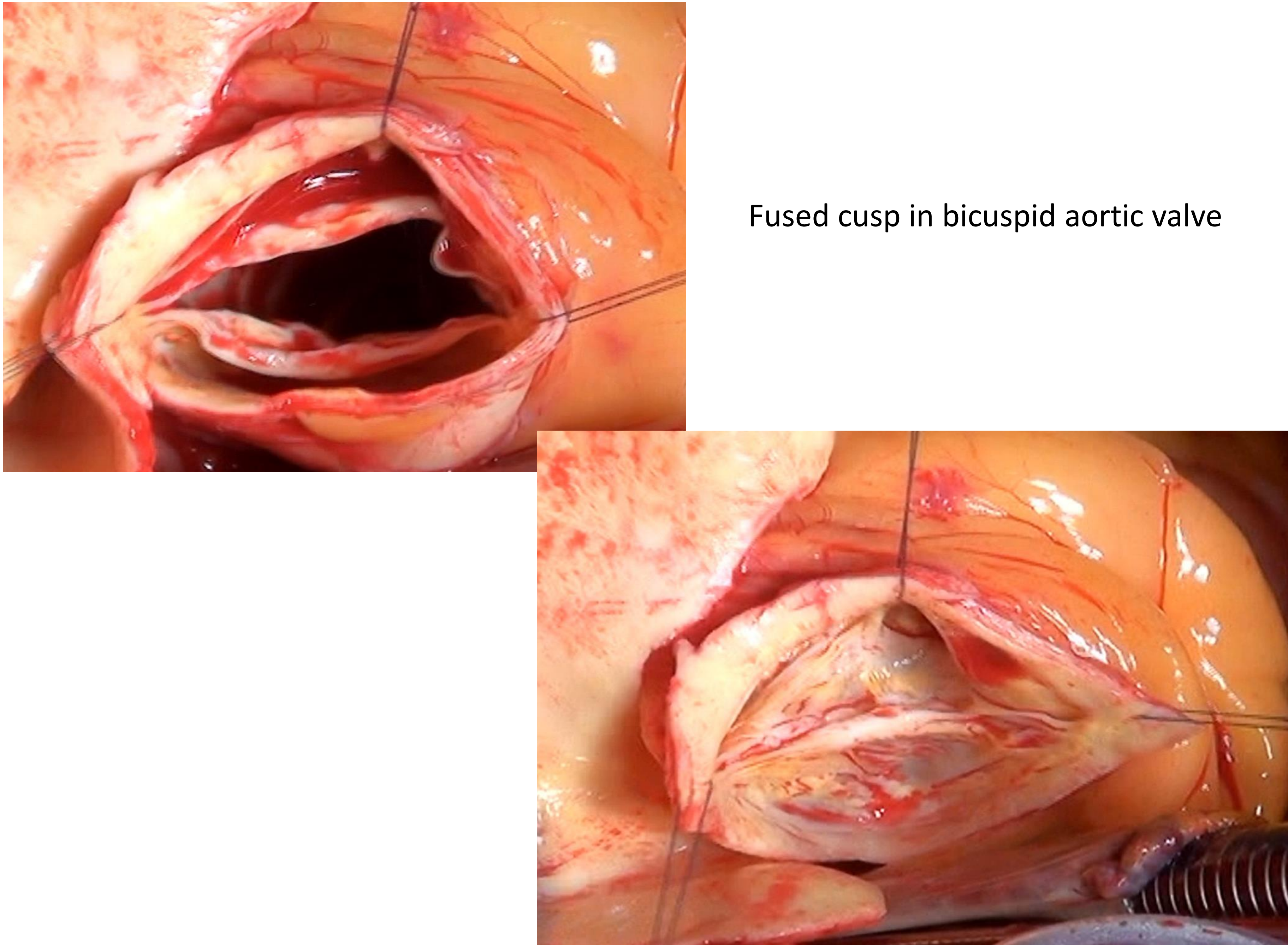

Fused cusp in bicuspid aortic valve

LEIPZIG-DALLAS

Echocardiographic **predictors of successful AV repair**

Localization and characterization of aortic valve pathology by 3D TEE

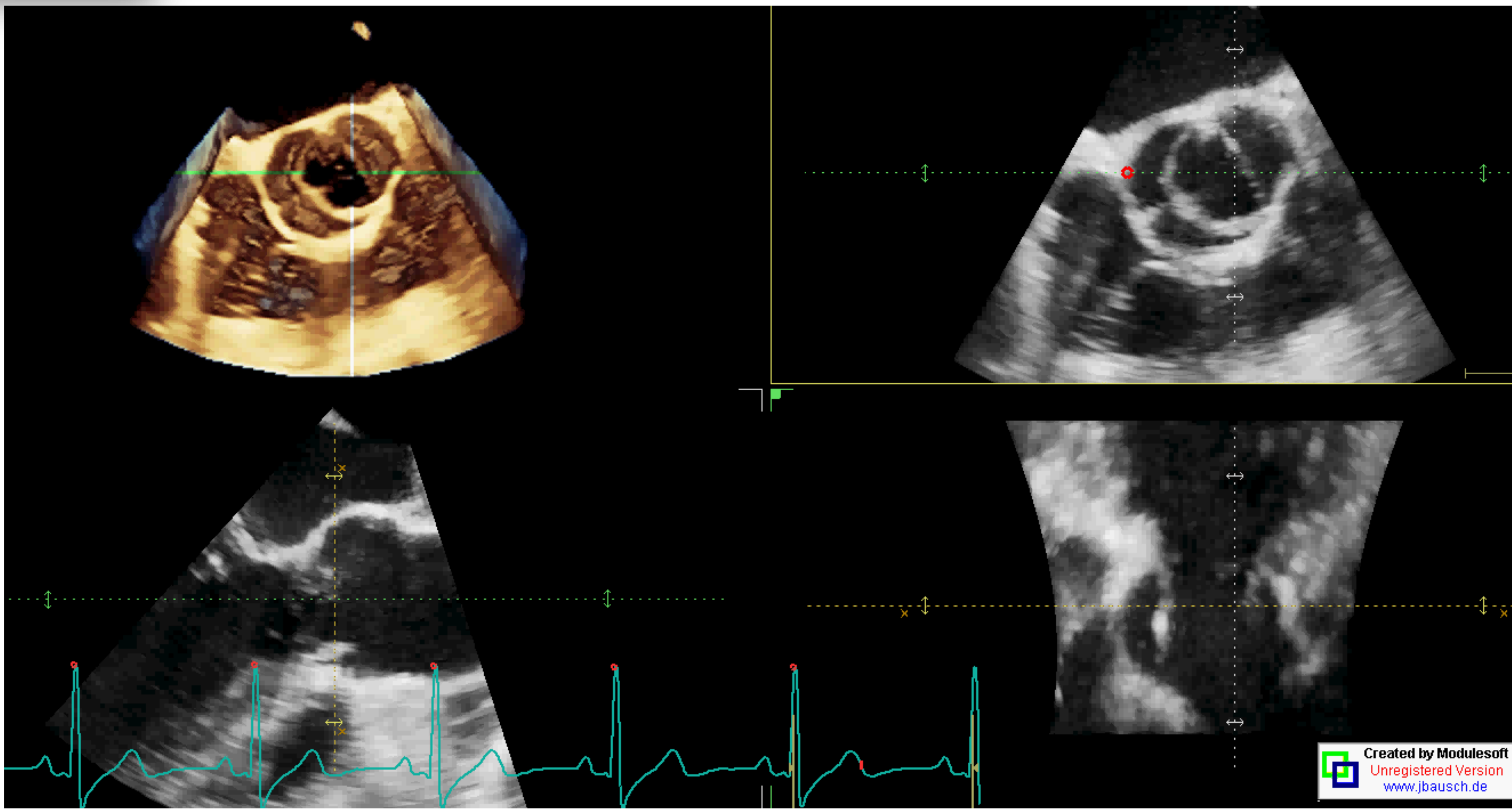

56 y, m, asymptomatic AR III


ELSEVIER

European Journal of Cardio-thoracic Surgery 38 (2010) 400–406

EUROPEAN JOURNAL OF CARDIO-THORACIC SURGERY

www.elsevier.com/locate/ejcts

Aortic root and cusp configuration determine aortic valve function☆

Benjamin Oliver Bierbach[a], Diana Aicher[a], Omar Abu Issa[a], Hagen Bomberg[a], Stefan Gräber[b], Petra Glombitza[a], Hans-Joachim Schäfers[a,*]

[a] Department of Thoracic and Cardiovascular Surgery, University Hospitals of Saarland, Kirrbergerstrasse 1, 66421 Homburg/Saar, Germany

[b] Institute for Medical Biometry, Epidemiology and Informatics, University Hospitals of Saarland, Homburg/Saar, Germany

Received 30 September 2009; received in revised form 19 January 2010; accepted 21 January 2010; Available online 12 March 2010

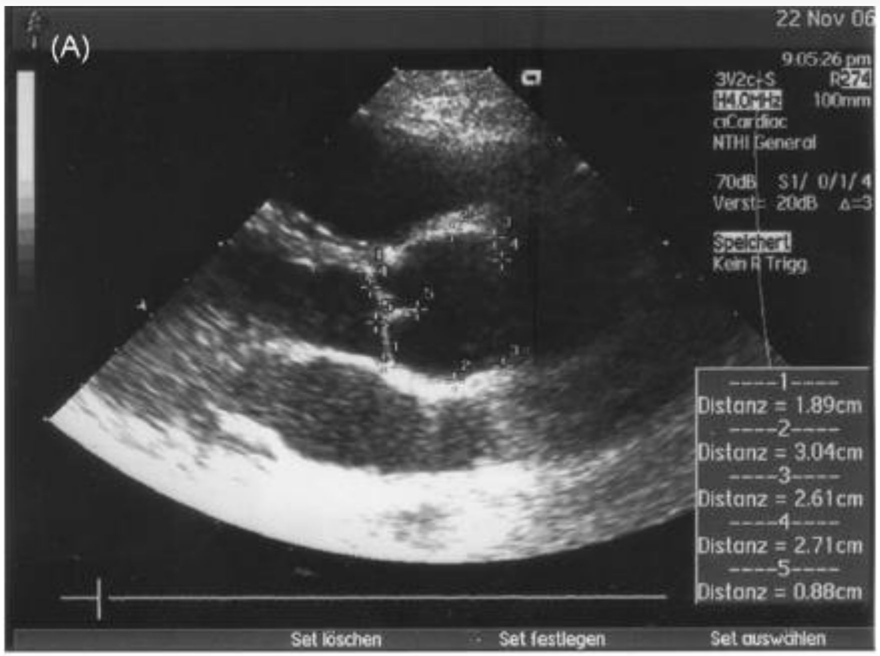

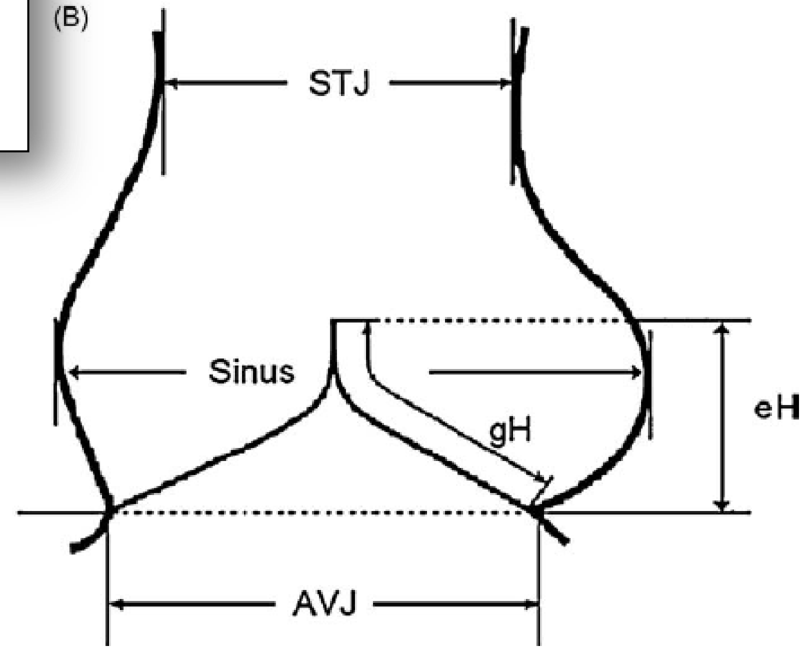

Fig. 1. Aortic root dimensions at different levels and effective height measured by transthoracic echocardiography in the long parasternal axis (A) and a schematic drawing (B). STJ: sinutubular junction; Sinus: maximum sinus diameter, gH: geometric height; eH: effective height; AVJ: aortoventricular junction.

Conclusions: Parameters of aortic root dimensions follow a seemingly constant pattern in humans of different sizes. Effective height has a constant relationship to root dimensions and body size. In AVR, normalisation of eH leads to a high probability of normal or near-normal aortic valve function.

LEIPZIG-DALLAS

Echocardiographic **predictors of successful AV repair**

Intraoperative surgical measurements

geometric height left

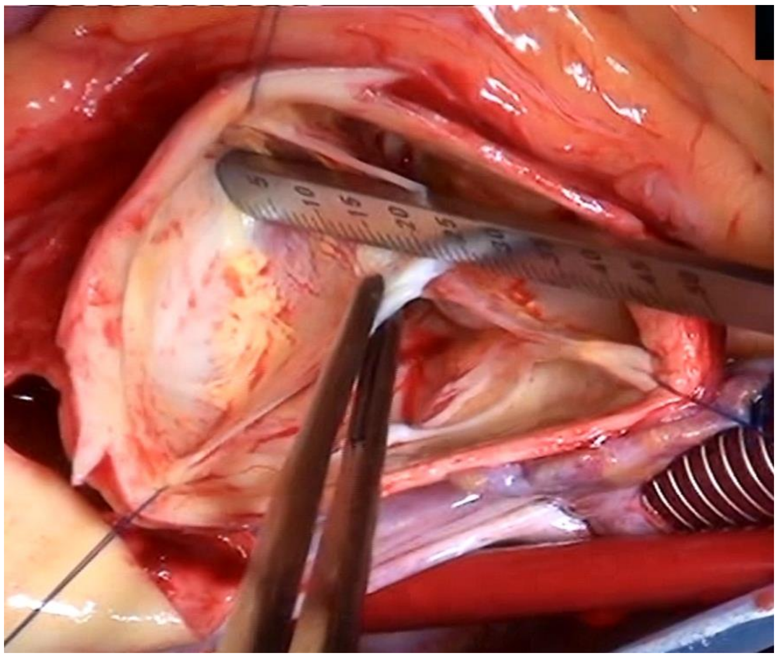

effective height left

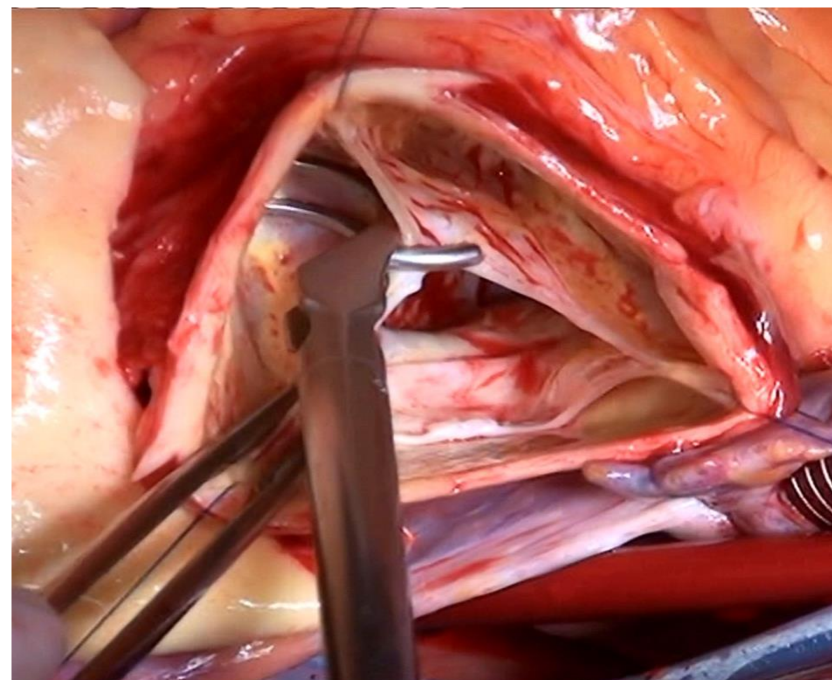

Reconstruction of the Aortic Valve and Root, Homburg
2013 May 15th/16th/17th Case 2
Prof. Schaefers

Echocardiographic **predictors of successful AV repair**

Measurement of the effective height for each aortic valve cusp by 3D TEE

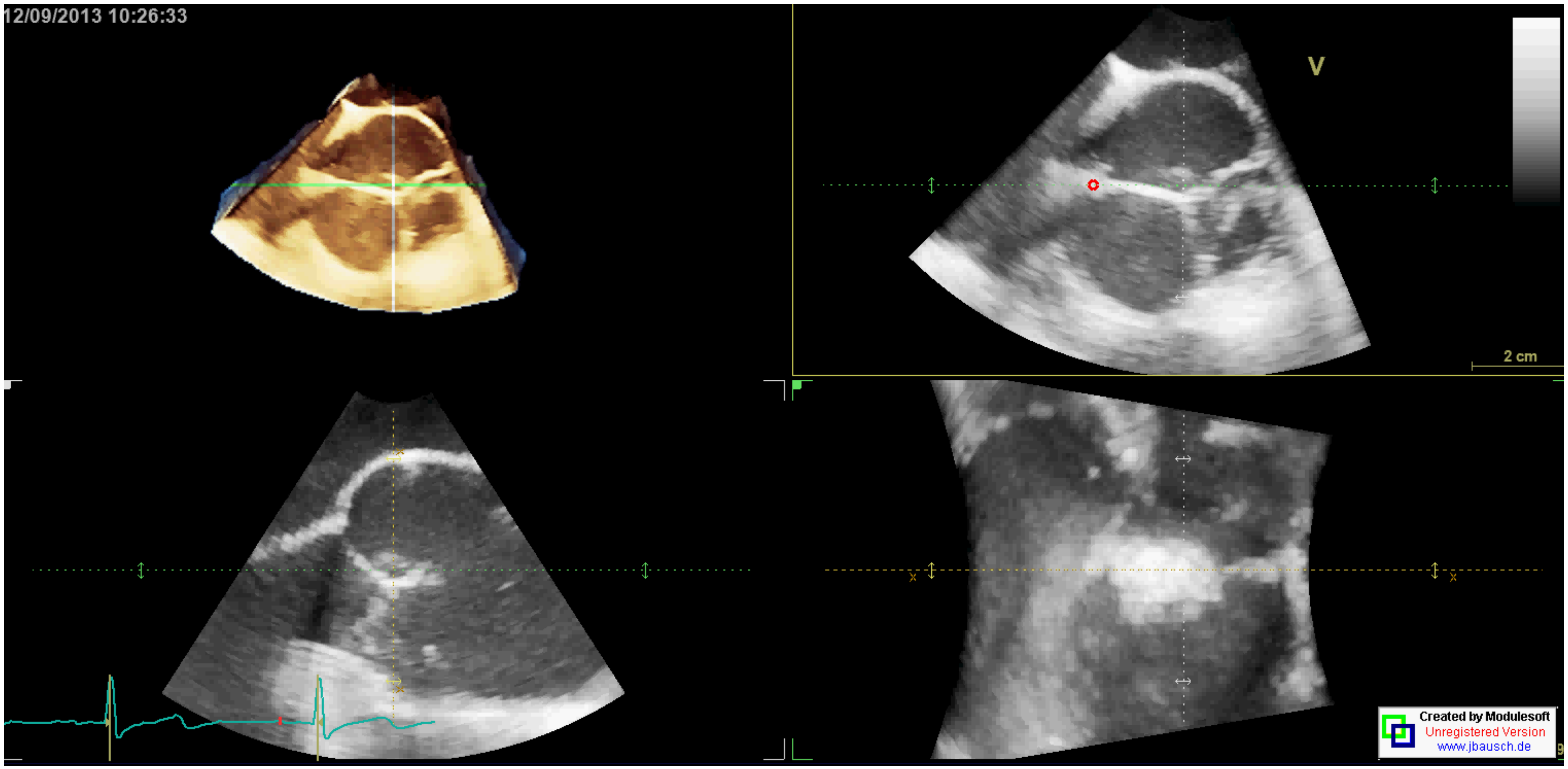

Reconstruction of the Aortic Valve
and Root, Homburg
2013 May 15th/16th/17th Case 3
Prof. Schaefers

Echocardiographic **predictors of successful AV repair**

Measurement of the effective height for each aortic valve cusp by 3D TEE

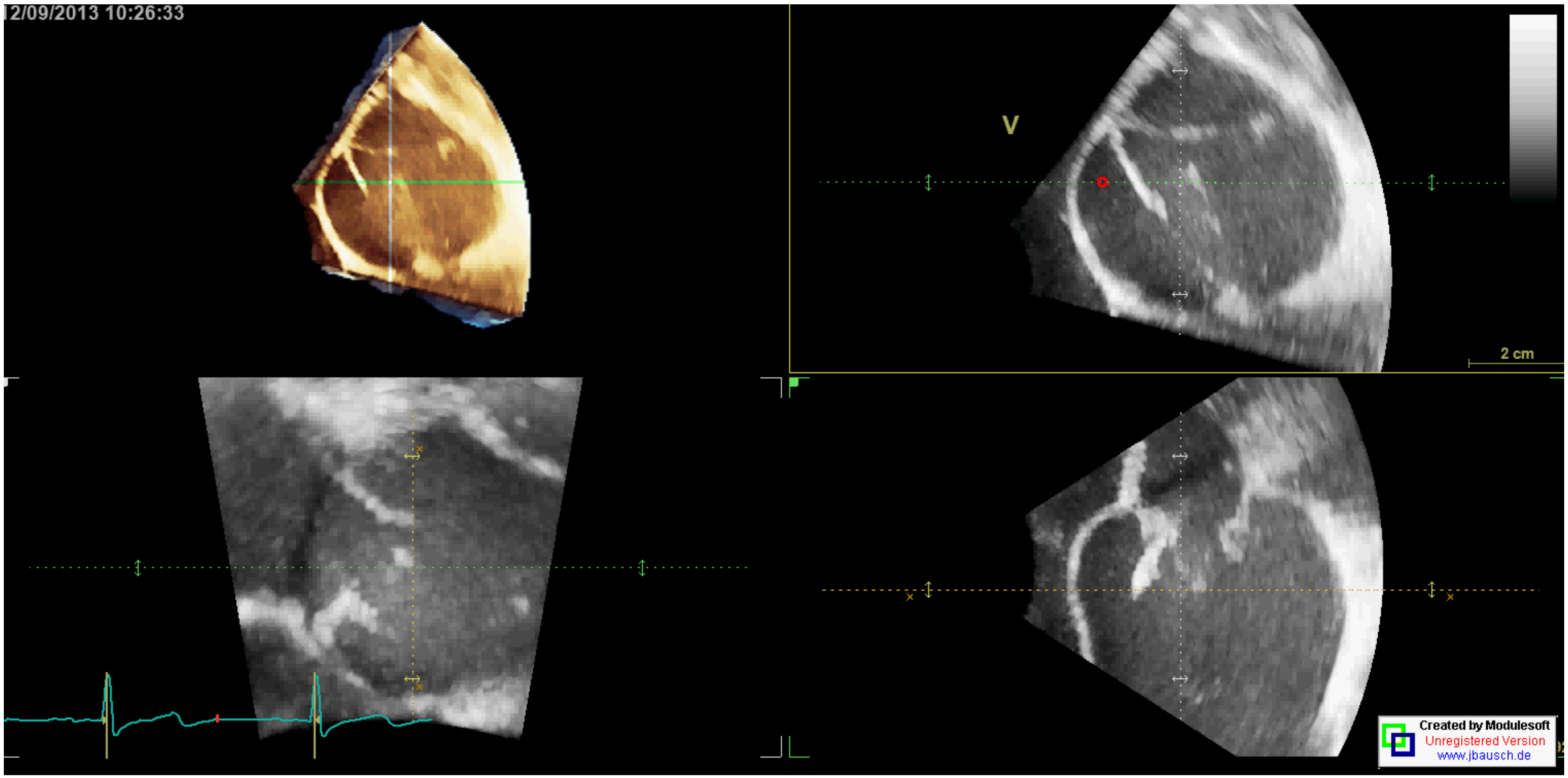

Reconstruction of the Aortic Valve and Root, Homburg
2013 May 15th/16th/17th Case 3
Prof. Schaefers

Left coronary cusp measurements not possible in 2D echo

Echocardiographic **predictors of successful AV repair**

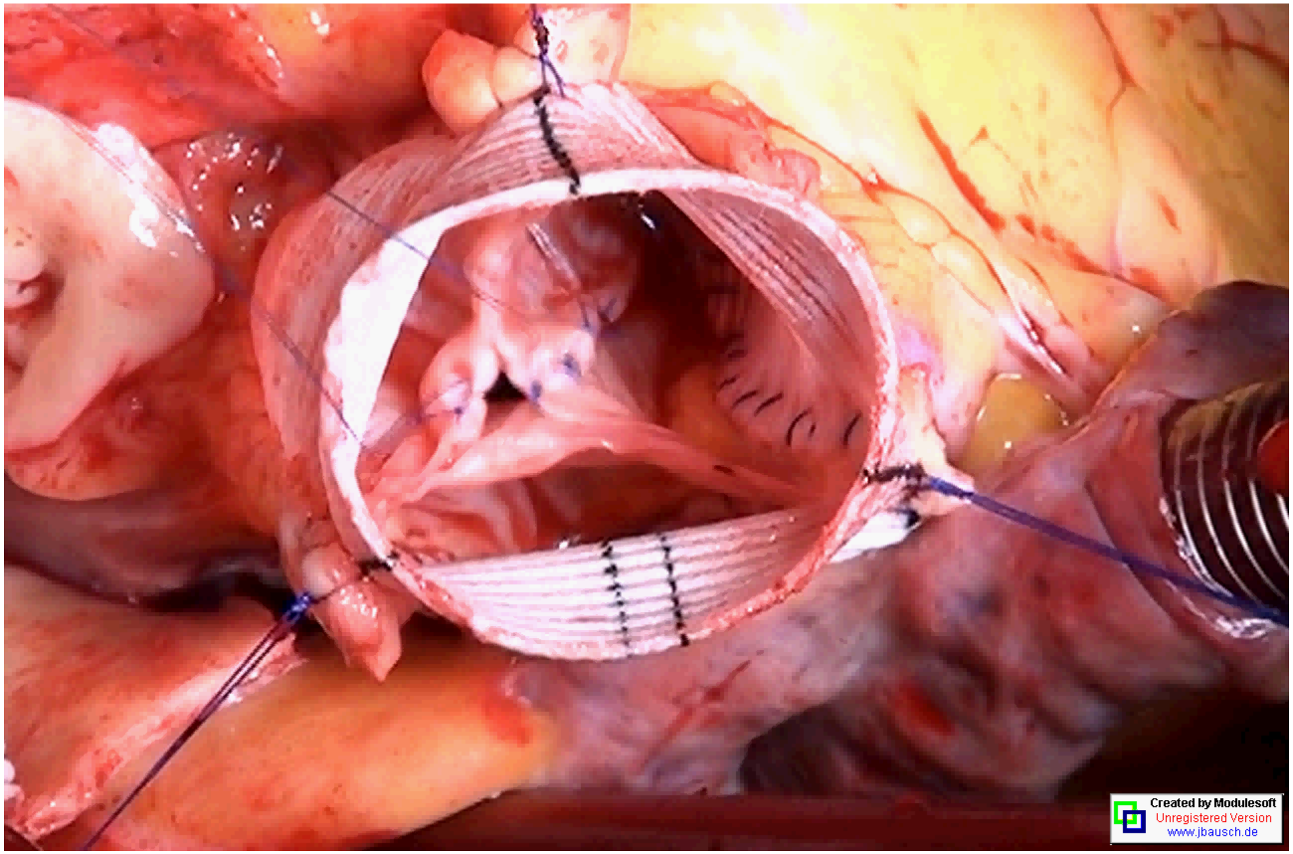

Reconstruction of the Aortic Valve
and Root, Homburg
2013 May 15th/16th/17th Case 3
Prof. Schaefers

Echocardiographic **predictors of successful AV repair**

Postoperative control after repair of aortic valve

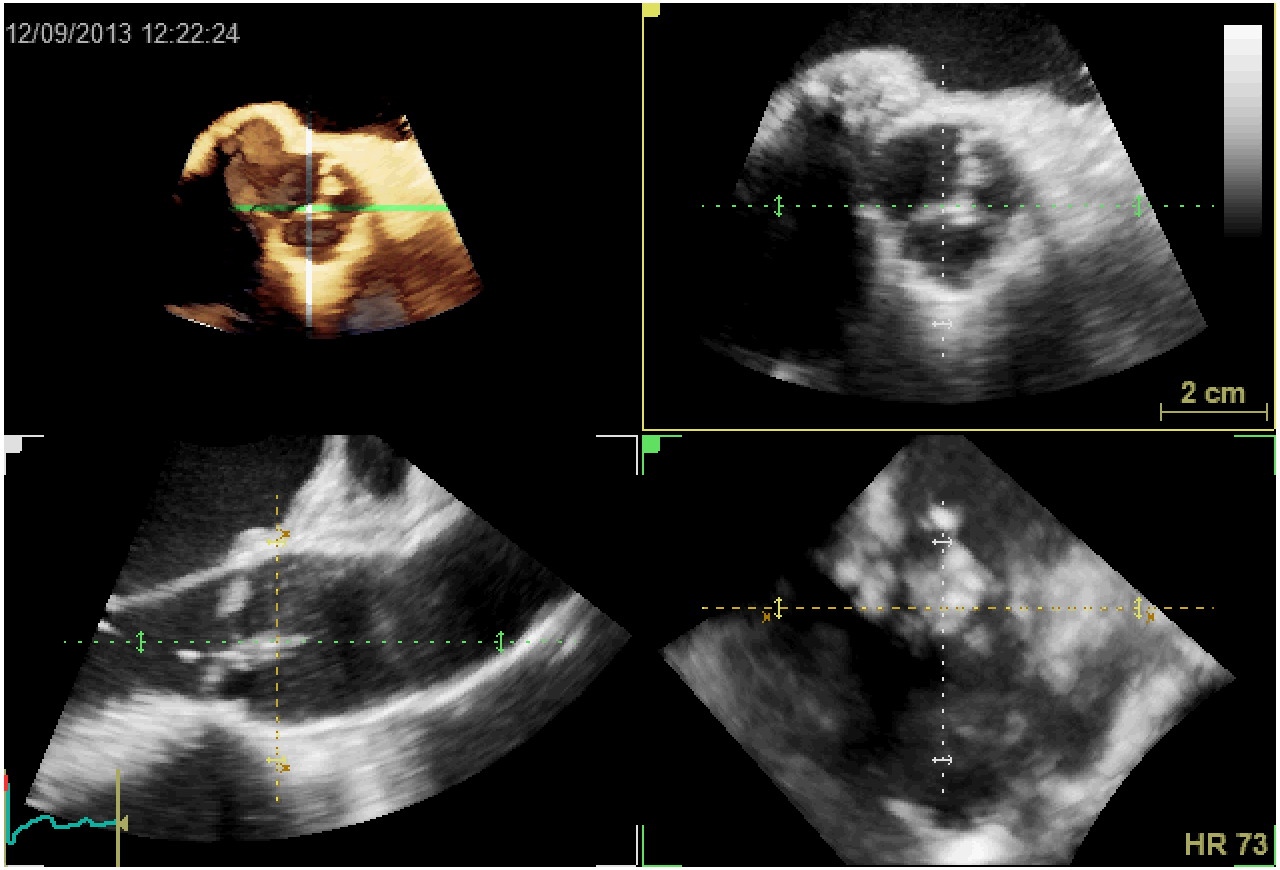

Reconstruction of the Aortic Valve
and Root, Homburg
2013 May 15th/16th/17th Case 3
Prof. Schaefers

Echocardiographic **predictors of successful AV repair**

Postoperative control after repair of aortic valve

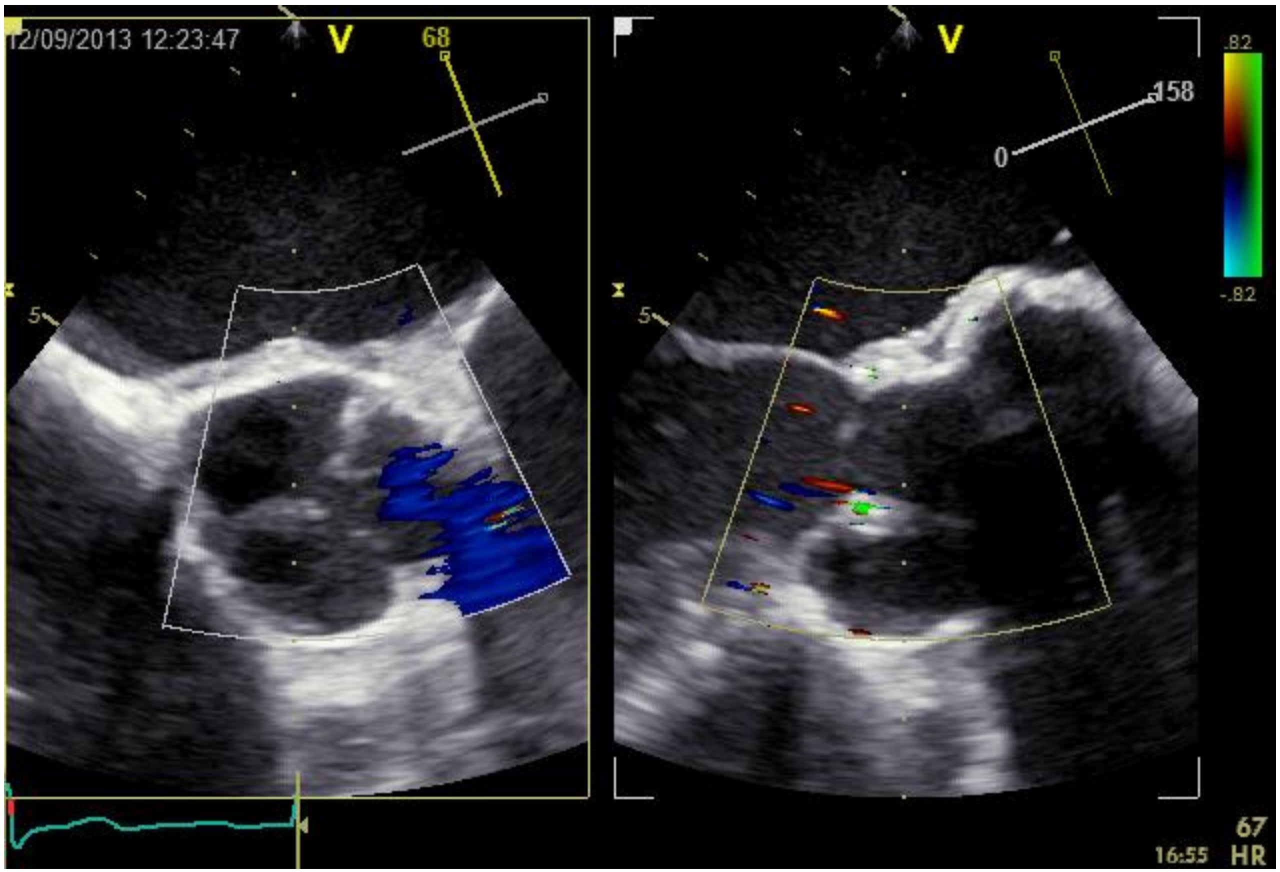

Reconstruction of the Aortic Valve
and Root, Homburg
2013 May 15th/16th/17th Case 3
Prof. Schaefers

S. R., 60 y, m; AI III/IV, NYHA I - II

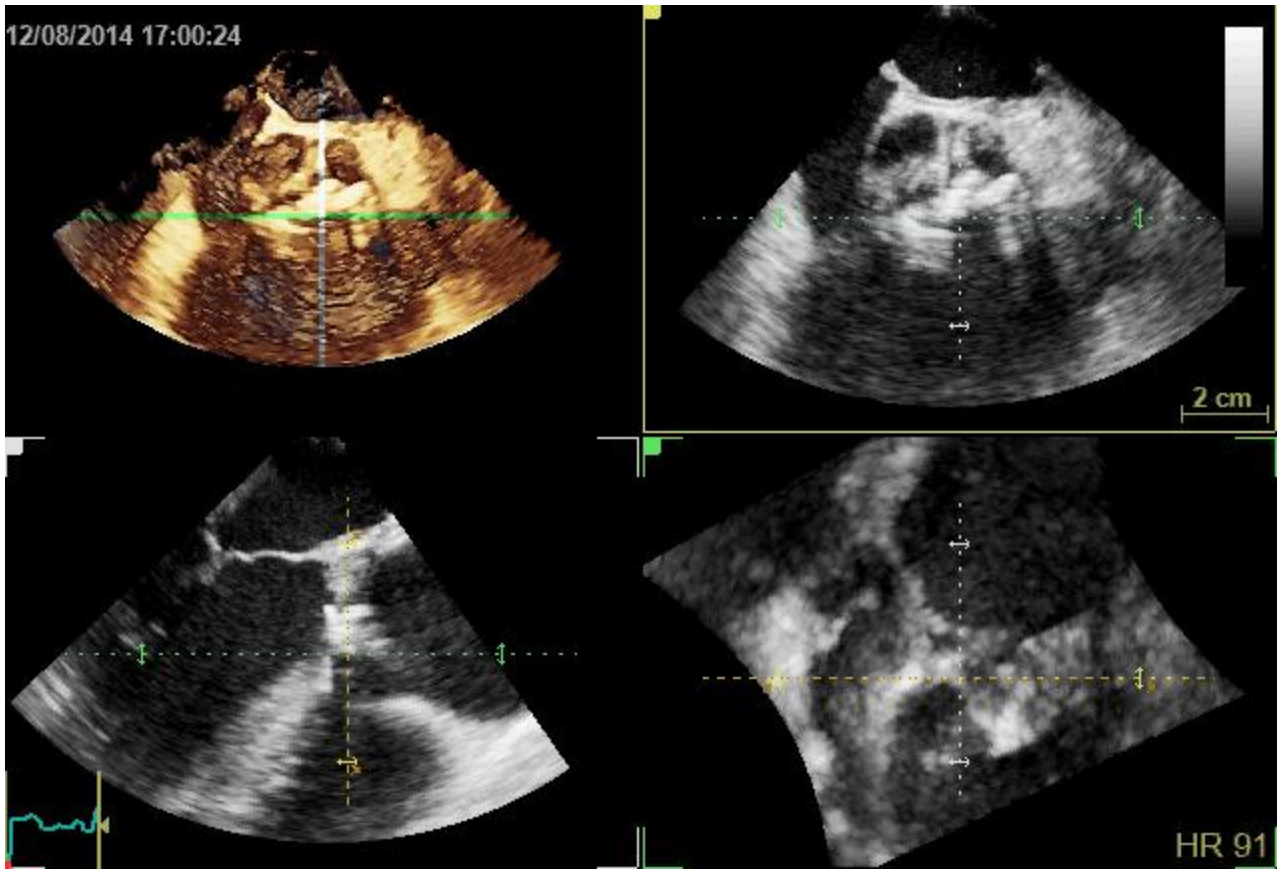

Bicuspid AV, calcified commissure (raphe) between rigtht and left coronary cusp

S. R., 60 y, m; AI III/IV, NYHA I - II

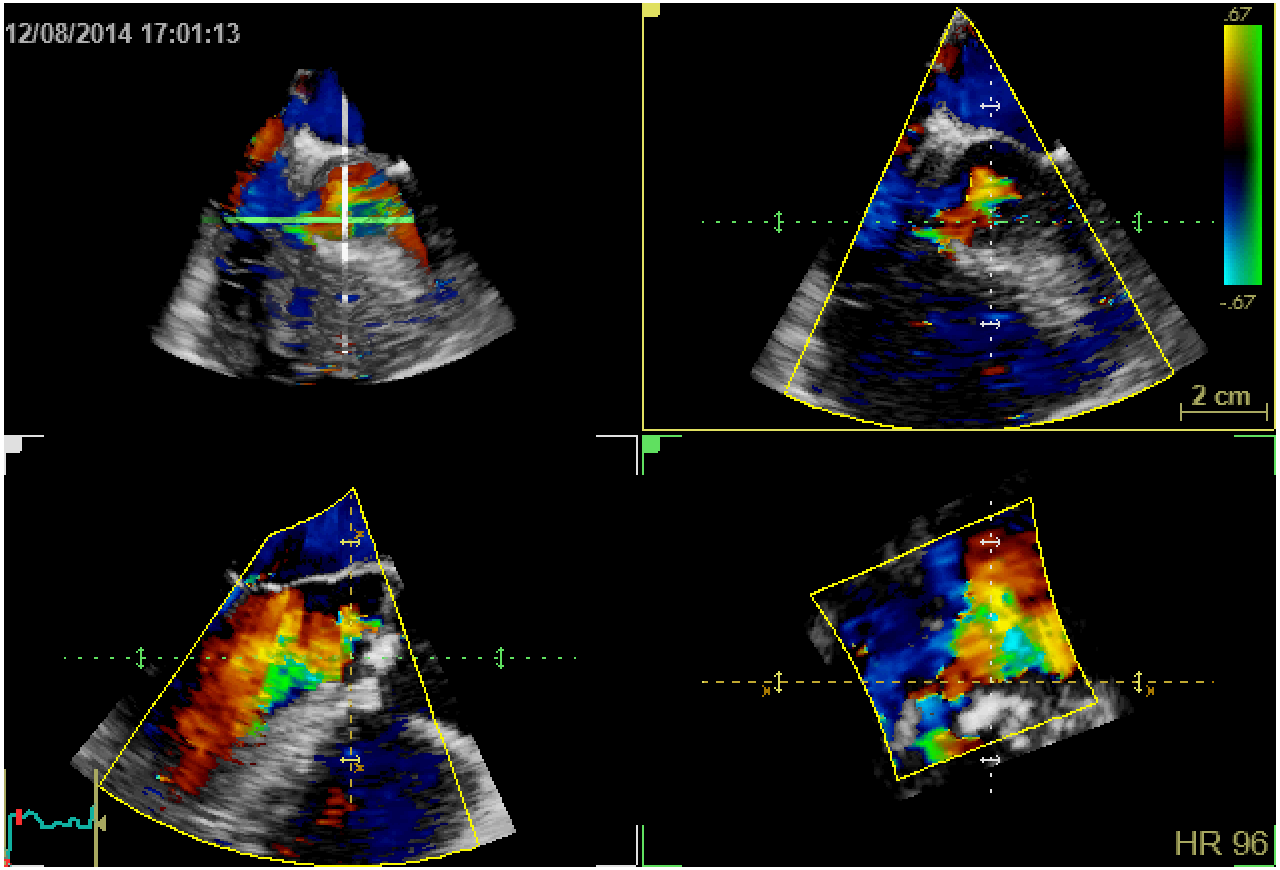

Bicuspid AV, calcified commissure (raphe) between rigtht and left coronary cusp

S. R., 60 y, m; AI III/IV, NYHA I - II

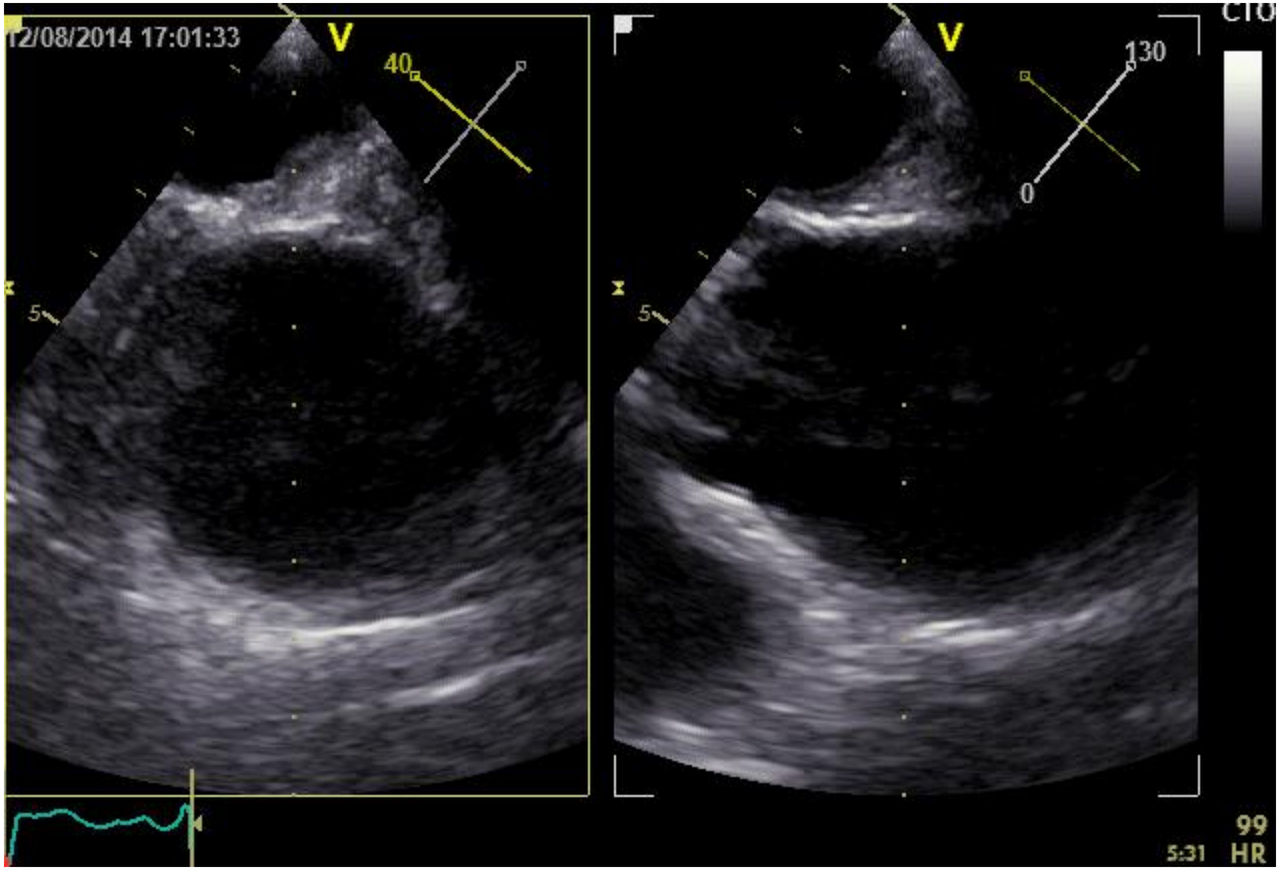

Bicuspid AV, calcified commissure (raphe) between rigtht and left coronary cusp

S. R., 60 y, m; AI III/IV, NYHA I - II

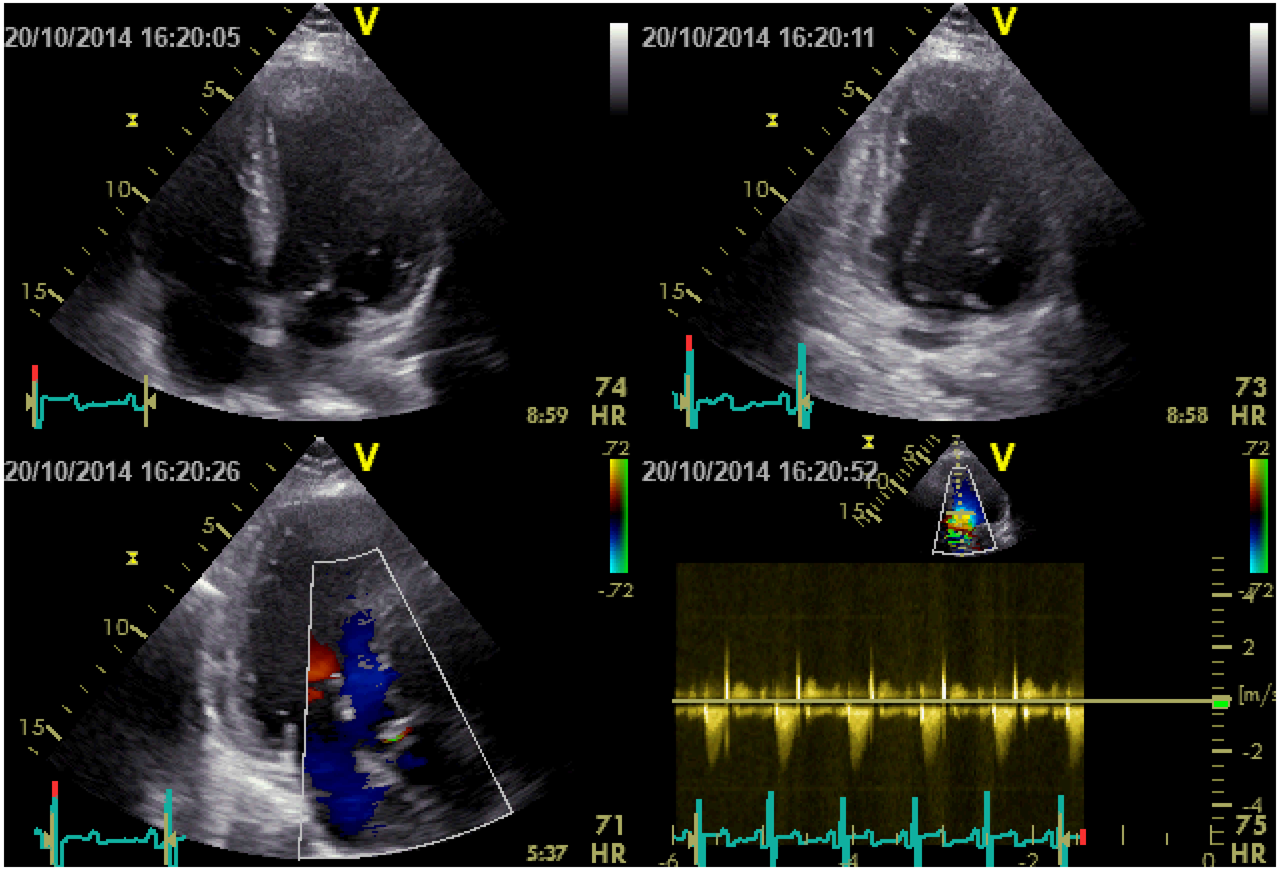

Bicuspid AV, calcified commissure (raphe) between rigtht and left coronary cusp

Postoperative no leak no stenosis

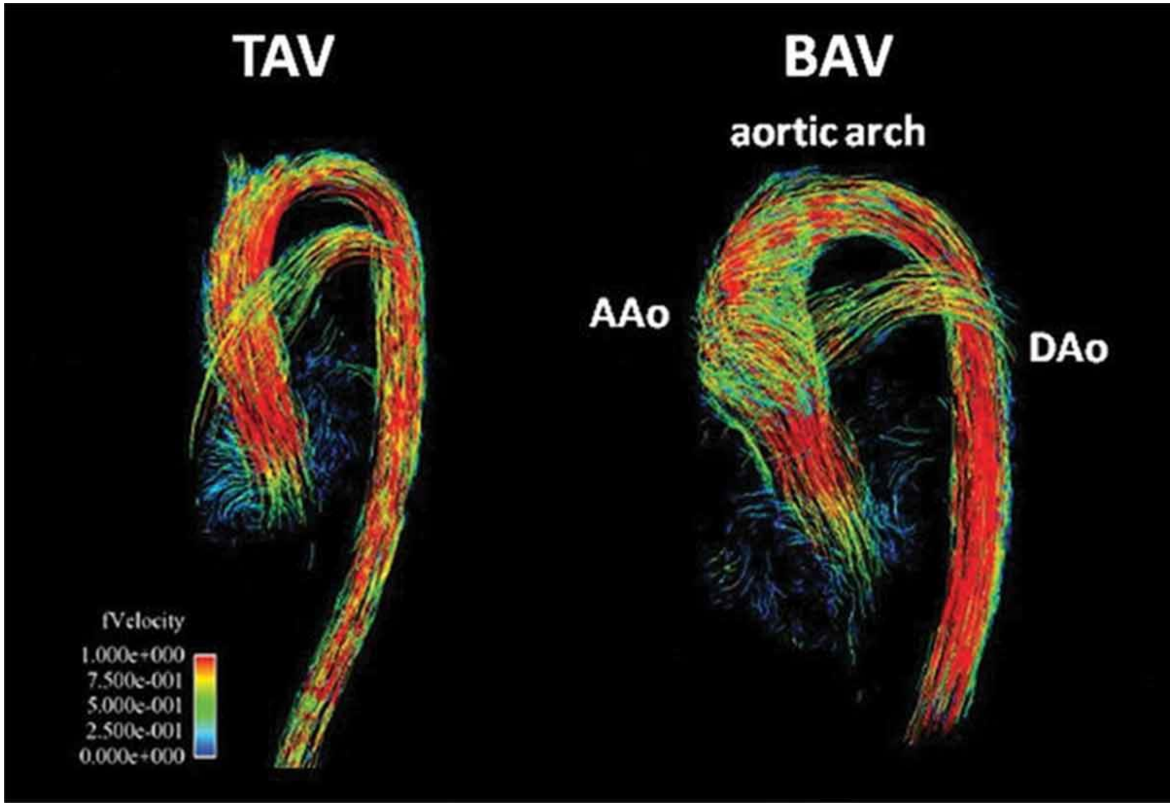

Figure 5. **4D flow MRI of the aortic valve and aorta**. Comparison of 4D flow MRI streamlines of the aortic flow in a patient with tricuspid aortic valve (TAV) and a patient with bicuspid aortic valve (BAV). Reproduced from Meierhofer *et al*. [66] with permission from the Oxford University Press.

Published in: Madelien V. Regeer; Michel I.M. Versteegh; Nina Ajmone Marsan; Jeroen J. Bax; Victoria Delgado; *Expert Review of Cardiovascular Therapy* **2016,** 14, 75-86.
DOI: 10.1586/14779072.2016.1109448

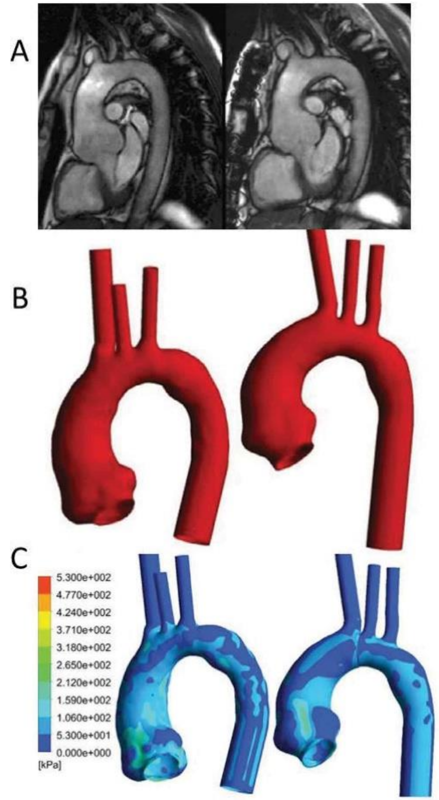

Figure 6. **Finite element model of the aortic root**. This example illustrates how finite element technology can evaluate the effects of personalized external aortic root support in a patient with aortic root disease due to Marfan syndrome. From cardiac magnetic resonance at baseline and after implantation of the personalized external aortic root support (panel A), the 3-dimensional models of the aortic root were reconstructed (panel B). Finite element analysis was applied to evaluate the stress distribution in the aortic wall (panel C). For all panels, left indicates baseline and right indicates post-intervention. Reproduced from Singh *et al*. [63] with permission from Elsevier.

Published in: Madelien V. Regeer; Michel I.M. Versteegh; Nina Ajmone Marsan; Jeroen J. Bax; Victoria Delgado; *Expert Review of Cardiovascular Therapy* **2016,** 14, 75-86.
DOI: 10.1586/14779072.2016.1109448

were assigned to 1 of 3 pathological categories on the basis of surgical inspection, as follows: 1) type I, dilation of aortic root (n = 20); 2) type II, leaflet prolapse with flail leaflet, transverse fibrous banc fenestration (n = 36); and 3) type III, restricted leaflet due to valve and calcifications (n = 14). Pre-operative TEE was cond within 3 months before surgery using the iE33 ultrasound s (Philips Medical Systems, Bensalem, Pennsylvania). 3D da were analyzed using novel 3D, knowledge-based, valve-mod software (Siemens Medical Solutions, Mountain View, California) (2). Regurgitant orifice height (ROH) was measured as the 3D perpendicular distance from the annular plane to the center of the 3 leaflet tips in end-diastolic frame (Fig. 1D).

In pre-operative clinical characteristics, there were no differences

0.001] and 0.93 [p < 0.001], respectively) in 2D and 3D TEE measurement parameters. The best cutoff values for types I and II were ROH ≥7 mm (sensitivity 100%, specificity 100%) and <4 mm (sensitivity 74%, specificity 94%), respectively.

The main accomplishment was successful quantitative 3D eval-

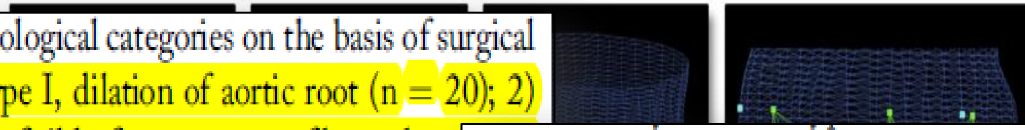

…s of aortic valve (**green points**), the 3 nadirs of cusp (**violet points**), and the 3 …llowing parameters were measured automatically (**A**) aortic root area: annulus …llow), RCC (**blue**), NCC (**violet**); (**C**) leaflet length: LCC leaflet (**yellow dotted** …fice height (**yellow arrow**). AVAp = aortic valve apparatus; L = left; LCC = left-

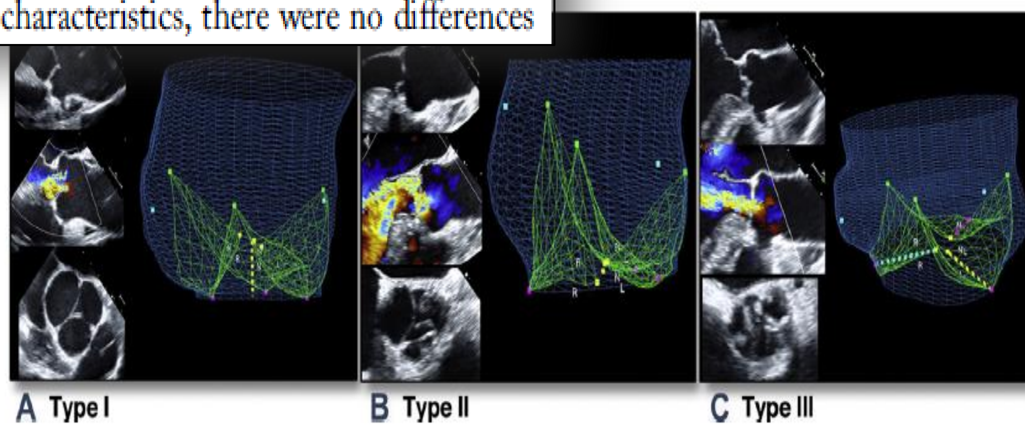

Figure 2. 2D TEE and Volume-Rendered 3D TEE Representations of AVAp in the 3 AR Types

(**A**) Type I, dilation of aortic root; (**B**) type II, leaflet prolapse of right-coronary cusp leaflet; and (**C**) type III, retraction of all leaflets. **Blue points**: coronary ostium, **green points**: aortic valve commissures, **violet points**: cusp nadirs, and **yellow points**: leaflet tips. 2D = 2-dimensional; 3D = 3-dimensional; AR = aortic regurgitation; TEE = transesophageal echocardiography.

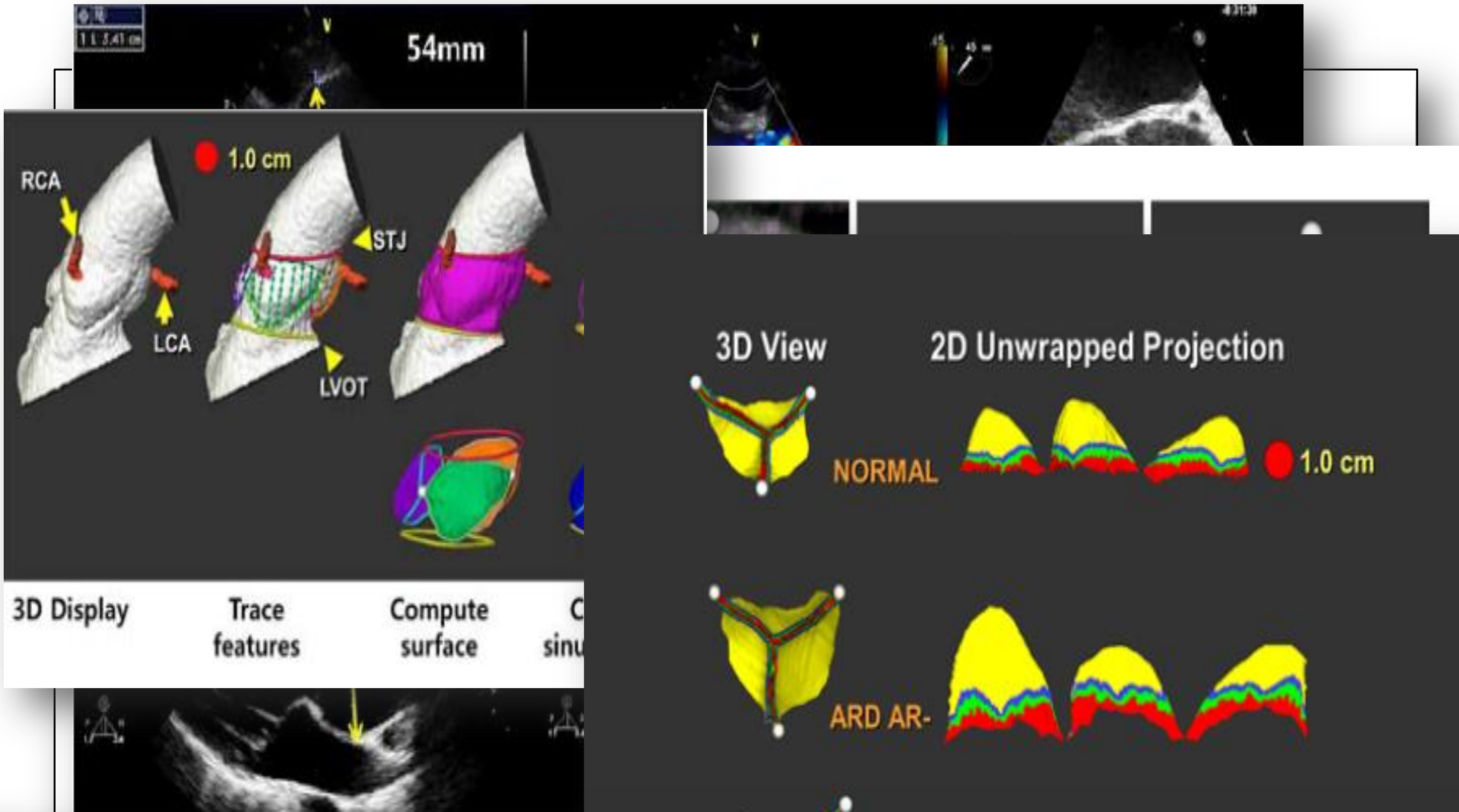

normals to 12.9±2.2 cm^2/m^2 in AR-negative and 15.2±3.3 cm^2/m^2 in AR-positive patients. However, the ratio of closed cusp surface area to maximal mid-sinus area, reflecting cusp adaptation, decreased from normals to AR-negative to AR-positive patients (1.38±0.20, 1.15±0.15, 0.88±0.15; $P<0.001$), creating the lowest coaptation area fraction. Cusp distensibility (closed diastolic versus open area) decreased from 20% in controls and AR-negative patients to 5% in AR-positive patients ($P<0.001$). Multivariate determinants of AR and coaptation area fraction reflected both sinus size and cusp-to-annular adaptation. ARD was also progressively asymmetrical with root size, and individual cusp surface areas failed to match this asymmetry.

valve adaptation and 3-dimensional relationships; understanding cusp adaptation mechanisms may ultimately provide therapeutic opportunities to improve such compensation. (*Circ Cardiovasc Imaging*. **2014;7:828-835.**)

la pratica dev' essere edificata sopra la buona teorica
(Practice must always be founded on sound theory)
Leonardo Da Vinci

Day 1

08.30	Arrival, registration	
09.00	Welcome and introduction	*H.-J. Schäfers*
09.45	Aortic regurgitation and aneurysm-Epidemiology and guidelines	*S. Ewen*
	BREAK	
10.30	Anatomy of aortic valve and root	*E. Lansac*
11.00	AV repair – the Homburg approach	*H.-J. Schäfers*
11.30	Why and when to repair the aortic valve	*D. Aicher*
	BREAK	
13.00	Videos root repair	*H.-J. Schäfers*
13.15	Echo assessment of AR and its mechanisms	*W. Fehske*
13.30	Results root repair	*D. Aicher*
14.00	3-dimensional echo in aortic valve repair	*W. Fehske*
14.30	Videos root repair II	*H.-J. Schäfers*
15.30	The AV junction in aortic repair	*E. Lansac*
16.00	Videos cusp repair	*H.-J. Schäfers*
17.30	Results of cusp repair	*D. Aicher*
18.00	Adjourn	

A practical approach

Wednesday, April 27th to Friday, April 29th, 2016